Rock Mechanics Bulletin 5 (2026) 100237

Contents lists available at ScienceDirect

Rock Mechanics Bulletin

journal homepage: www.keaipublishing.com/en/journals/rock-mechanics-bulletin

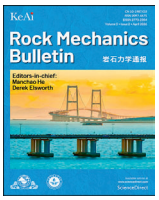

Review Article

Recent advancements for cement grout diffusion mechanisms within rock fractures

Haizhi Zang, Shanyong Wang*

School of Engineering, University of Newcastle, University Drive, Callaghan, NSW, 2308, Australia

ARTICLE INFO

Keywords:
Rock fracture grouting
Grout diffusion
Fracture networks
Non-Newtonian grout
Numerical modelling

ABSTRACT

Understanding cement grout diffusion in rock fractures is crucial for rock engineering, yet grouting faces significant challenges due to fracture network heterogeneity and grout's complex non-Newtonian rheology. This study critically reviews recent theoretical, experimental, and numerical advancements to comprehensively understand cement grout diffusion mechanisms within rock fractures. It begins by discussing theoretical foundations, encompassing both continuum and particulate views in single fractures, while also highlighting limitations in extending these simplified concepts to fracture networks and defining robust stop criteria. Subsequently, the article details developments in experiments, including novel apparatus and advanced monitoring techniques. These enable controlled observation of grout diffusion in artificial or simulated fractures, providing crucial insights into the impact of fracture complexities (e.g., fracture roughness, two-phase flow) on grout patterns and sealing efficiency. These laboratory tests also inform the development of practical stop criteria by revealing actual grout behaviour under various conditions. Complementary numerical methods offer a distinct advantage by providing dynamic, continuous solutions for complex fracture networks that are otherwise intractable. Collectively, these diverse approaches bridge critical knowledge gaps, from fundamental principles to real-world complexities, and facilitate cross-scale validation. The review concludes by identifying persistent challenges, such as integrating multi-scale descriptions and simulating true field complexities, and outlines future research directions to understand grout diffusion mechanisms.

1. Introduction

Rock fracture grouting is a crucial technique in rock engineering for enhancing the integrity and stability of rock masses, as well as effectively controlling groundwater flow in a diverse range of projects. This essential method has been widely used in critical underground infrastructure, including dam foundations, tunnels, and mining excavations, and is particularly vital for achieving high sealing requirements in facilities such as nuclear waste repositories and gas storage caverns (Duan et al., 2024; Kang et al., 2023; Si et al., 2025). The primary objectives of grouting are to reduce rock mass permeability and improve its mechanical properties through injecting specialized grout materials into rock discontinuities. However, rock masses are highly heterogeneous, where fractures exhibit considerable variability in orientation, size, aperture, and roughness (Lei et al., 2021). The grout itself also often behaves as a non-Newtonian fluid (such as Bingham or Herschel-Bulkley fluids) with rheological properties that are time-dependent due to hydration and flocculation (Zang et al., 2024). Consequently, complex grout diffusion mechanisms within fractured rock masses have posed significant challenges to accurate prediction and control.

To enhance the understanding of grout diffusion mechanisms within rock fractures, researchers have used a combination of theoretical, experimental, and numerical methods. Theoretical models typically simplify grout flow in idealized geometries (Nazempour and Majdi, 2021), such as channels or radial patterns between parallel plates (Shamu et al., 2020). These models often consider grout a non-Newtonian fluid (Liu et al., 2020a; Zou et al., 2020a), allowing for the derivation of analytical solutions for parameters like penetration length, velocity, and pressure distribution (Han et al., 2021; Shamu et al., 2021). Simultaneously, experimental investigations use simulated fractures and visualisation platforms to observe grout diffusion in real time (Xiang et al., 2025). These studies explore crucial factors such as grout penetrability (Nejad Ghafar et al., 2017), filtration (El Mohtar et al., 2022), the influence of fracture roughness (Duan et al., 2025), and

* Corresponding author.
E-mail address: Shanyong.Wang@newcastle.edu.au (S. Wang).
Peer review under the responsibility of Chinese Society for Rock Mechanics & Engineering.

https://doi.org/10.1016/j.rockmb.2025.100237
Received 22 April 2025; Received in revised form 10 July 2025; Accepted 6 August 2025
Available online 22 August 2025

flowing water conditions (Zhang et al., 2025). Complementing these approaches, advanced computational methods model grout propagation in complex two-dimensional and three-dimensional fracture networks (Zou et al., 2019, 2020b). These simulations frequently incorporate non-Newtonian rheology (Ortega and Vergara, 2024) and hydro-mechanical coupling (Latham et al., 2013; Xiao et al., 2019) to accurately represent grout diffusion patterns.

Despite these advancements, significant challenges persist in rock fracture grouting. A primary obstacle is the continued reliance on empirical knowledge, largely due to the inherent unpredictability and heterogeneity of geological conditions in practical applications (Ma et al., 2025). Existing theoretical models often oversimplify rock fractures by assuming idealized geometries, which fail to adequately account for critical features (i.e., roughness, tortuosity, variable apertures) (Wang et al., 2020). Furthermore, a comprehensive understanding is hindered by complex grout-rock mass interactions, including phenomena such as pressure filtration (Ghafar et al., 2017a; Lu et al., 2020) and the time-dependent, spatiotemporal variations in grout properties (Zou et al., 2018). Additionally, the precise patterns of grout distribution at fracture intersections are not yet fully understood (Sun et al., 2023). These unresolved issues highlight the urgent need for more efficient and accurate methods for grout design, monitoring, and quality assessment in modern rock engineering.

The review aims to: 1) Summarise advancements and challenges in theoretical grout diffusion mechanisms, exploring both continuum and particulate views. 2) Review developments in experimental attempts and advanced monitoring techniques or apparatus for observing grout flow in rock fractures. 3) Present advancements in numerical modelling of grout flow in fracture networks. This multi-method approach is critical: theoretical models establish foundational principles, experiments validate these in controlled environments, and numerical models extend understanding to realistic, complex, multi-scale scenarios. This review begins with an in-depth discussion on current theoretical grout diffusion mechanisms, covering continuum and particulate views, diffusion within complex fracture networks, and various grout stop criteria. Subsequently, it details laboratory-scale observations in parallel plate tests and rough fractures, as well as innovations in monitoring and testing apparatus. The review then delves into advanced numerical modelling of grout flow in fracture networks, exploring recent insights from different computational methodologies, and associated challenges and improvements.

2. Advancements and challenges in theoretical grout diffusion mechanisms

2.1. Diffusion mechanism in a single fracture

Cement grouting involves a mixture of granular materials, water, and various additives. Understanding grout diffusion through rock fractures can be approached from two distinct perspectives: as a continuous fluid (continuum view) or as a hybrid phase of discrete grout particles suspended in a carrier fluid (particulate view). While each of these scales offers unique insights into the underlying diffusion phenomena, a quantitative connection between the two remains largely unexplored. This section delves into how the diffusion mechanism is determined through these differing scales and attempts to establish their interconnection.

2.1.1. Continuum view

2.1.1.1. Grout rheological models. Simplifying grout as a homogeneous fluid is essential for integrating its grout rheology into continuum flow equations. Grout rheological models define how grout deforms and flows under stress. Common rheological models for grout include linear models (such as Bingham plastic model) and nonlinear models (such as Herschel-Bulkley model and Power-law model). The Bingham plastic model describes a linear relationship between shear stress and shear rate after the yield stress is overcome:

$$\tau = \tau_0 + \mu_p \frac{\mathrm{d}u}{\mathrm{d}y}, \text{ for } |\tau| > \tau_0 \tag{1}$$

$$\frac{\mathrm{d}u}{\mathrm{d}y} = 0, \text{ for } |\tau| \le \tau_0 \tag{2}$$

where τ is the shear stress, τ_0 is the yield stress, μ_p is the plastic viscosity, and $\frac{\mathrm{d}u}{\mathrm{d}y}$ is the shear rate. Power-law model describes the following nonlinear relationship between shear stress and shear rate (Lavrov, 2023):

$$\tau = K\left(\frac{\mathrm{d}u}{\mathrm{d}y}\right)^n \tag{3}$$

where K is the consistency index, and n is the flow behaviour index. Herschel-Bulkley model extends this to a yield stress flow behaviour after yielding (Lavrov, 2023):

$$\tau = \tau_0 + K\left(\frac{\mathrm{d}u}{\mathrm{d}y}\right)^n, \text{ for } |\tau| > \tau_0 \tag{4}$$

$$\frac{\mathrm{d}u}{\mathrm{d}y} = 0, \text{ for } |\tau| \le \tau_0 \tag{5}$$

Fig. 1 compares the schematic curves of different rheological models. The Power-law model accounts for the changes in "apparent viscosity" during the flow, i.e., increased viscosity ($n > 1$, shear thickening behaviour) or decreased viscosity ($n < 1$, shear thinning behaviour) as it flows faster, which is more suitable for most chemical grout in which flow resistance outperforms initial resistance (Liang et al., 2019). The Herschel-Bulkley model is highly versatile and widely used because it can accurately represent a broad spectrum of non-Newtonian fluids, including many types of grouts. It provides a more comprehensive description of the initial resistance to flow (Zou et al., 2024). This makes it particularly useful for modelling grout injection into complex fracture networks where both yield stress and shear-rate-dependent viscosity are important. A common issue is their prediction of infinite apparent viscosity at initial grout flow (Hassler et al., 1992). This can be addressed using alternative models such as the Carreau model (Hao et al., 2023), or regularized stress-shear rate curves to approximate the Bingham or Herschel-Bulkley model (Burgos et al., 1999; Papanastasiou and Boudouvis, 1997).

2.1.1.2. Thixotropy and flow initiation. A fundamental complexity in grout diffusion is the time-dependent nature of its grout rheological properties, especially for cement-based grouts, primarily due to hydration and thixotropy (Roussel et al., 2019). Hydration, the chemical

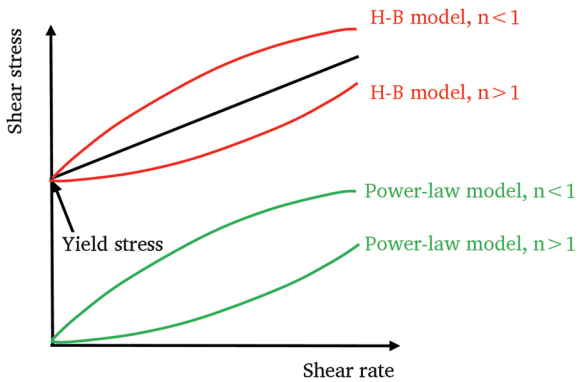

Fig. 1. Rheological behaviour of grout with different models.

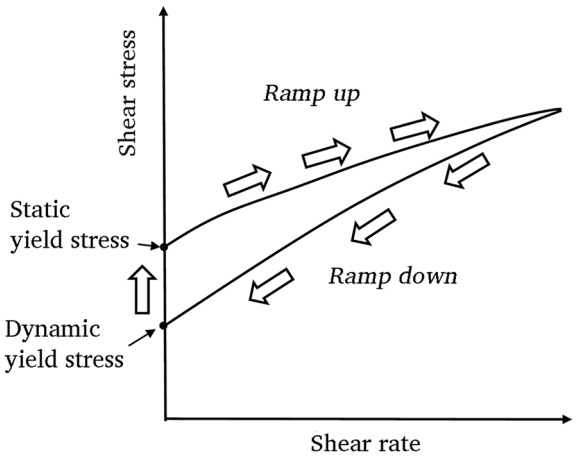

Fig. 2. Illustration of thixotropic grout behaviour, showing static and dynamic yield stress.

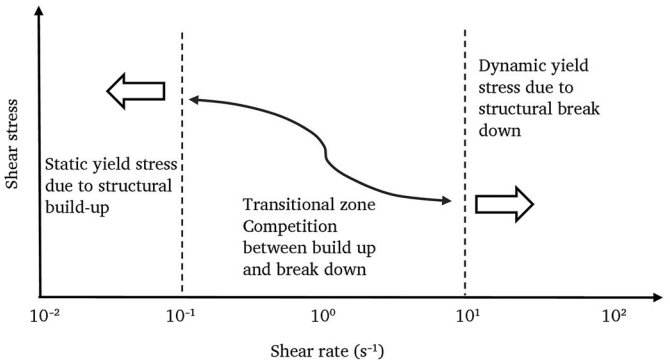

Fig. 3. Evolution of shear stress under constant applied shear, modified after (Rahman et al., 2017).

reaction of cement with water, causes hardening, with intensity affected by resting time and temperature. Thixotropic grout exhibits shear thinning (decreasing viscosity under continuous shear) and recovers its structure when stress is removed. Fig. 2 depicts typical stress-shear rate hysteresis curves of grout thixotropy. When grout is stirred or pumped (increasing shear rate), its resistance to flow (viscosity) decreases. If the shear rate is decreased to a full stop, its viscosity gradually increases. The time-varying viscosity and yield stress significantly influence grout propagation length, pressure distribution, and overall sealing effectiveness. Many traditional models often assume constant grout properties, which can limit their accuracy in real-world scenarios.

A critical shear stress or shear strain is often defined to determine the flow initiation of grout. The threshold must be greater than the stress or deformation required to break down the structural network of grout materials, which is typically represented as a yield stress or yield strain. However, the threshold is not a constant and changes with not only time (due to hydration) but also shear history (due to thixotropy). This imposes great challenges for analytical analysis of grout flow behaviour. For example, two types of yield stress are typically measured: static and dynamic (in Fig. 2). The choice of which yield stress to consider often depends on the flow history and the current state of the material (Larson and Wei, 2019). For instance, when starting to pump grout that has been at rest, the static yield stress might be more relevant, while the dynamic yield stress could be more important when considering the cessation of flow during pumping. Furthermore, instead of a critical level, Rahman et al. (2017) revealed that there is a transition from static to dynamic flow (in Fig. 3). After the initial breakdown, the grout transitions into a dynamic flow regime. In this phase, the rheological behaviour is often described by models such as the Bingham plastic or Herschel-Bulkley model, where the shear stress is related to the shear rate (and a dynamic yield stress). The dynamic yield stress is typically lower than the static yield stress because the structure is continuously being broken down by the ongoing shear. A spectrum of critical strain is also proven to exist due to different intensity of early hydration products (Zang et al., 2024).

2.1.1.3. Yield and plug flow. Continuum governing equations of grout flow within a single fracture are typically derived from Navier-Stokes (N-S) equations. Benefitting from the geometric simplicity of a narrow, oriented fracture, some necessary assumptions can be made to simplify the N-S equations into explicit analytical solutions, often under the following general assumptions:

1) Incompressible fluid: the density of grout does not change significantly with pressure or temperature during flow, which is a common approximation for grout due to fluid's negligible compressibility compared to gases (Park, 2020).
2) Steady laminar flow: the velocities, pressure and stress at any point in space do not change with time, and this assumes a stable state when the applied injection pressure is constant (Lavrov, 2023).
3) Negligible inertial terms: convective and unsteady terms in the momentum equations are insignificant compared to the pressure gradient and viscous terms, which is an effective approximation considering the low Reynolds number during grout flow (Zou et al., 2020b).
4) Lubrication approximation: no pressure variation across the fluid thickness, this is the most prominent assumption based on the fact that the geometric aperture of fracture is significantly smaller than the propagation length in the flow direction, which greatly simplifies the flow equations (Park and Lim, 2023).
5) Two-dimensional flow: no variations in flow properties across the width, which is a geometric simplification that reduces the complexity from 3D to 2D for simplified analytical solutions (Zou et al., 2019).

It is noted that the above assumptions can contradict to several applications, and they need to be cautiously checked before stepping into the derivation. The above assumptions reduce the N-S equations to the following flow equations (Liu and Park, 2020):

Cartesian coordinate system

$$\text{Mass conservation } \frac{\partial u_x}{\partial x}+\frac{\partial u_z}{\partial z}=0 \tag{6}$$

$$\text{Momentum conservation (along the } x-\text{direction)} -\frac{\partial p}{\partial x}+\frac{\partial \tau_{xz}}{\partial z}=0 \tag{7}$$

Polar coordinate system

$$\text{Mass conservation} \frac{\partial u_r}{\partial r}+\frac{u_r}{r}+\frac{\partial u_z}{\partial z}=0 \tag{8}$$

$$\text{Momentum conservation (along the } r-\text{direction)} -\frac{\partial p}{\partial r}+\frac{\partial \tau_{rz}}{\partial z}=0 \tag{9}$$

$$\text{Momentum conservation (along the } z-\text{direction)} -\frac{\partial p}{\partial z}=0 \tag{10}$$

where x or r is the primary flow direction and z is perpendicular to the primary flow direction, p is the pressure, u_i is the velocity. The shear stress τ in Eqs. (7) and (9) cannot be solved for velocities without a rheological model that relates the shear stress to the shear rate. That is where different governing equations for various type of grout can be developed.

The yield behaviour of cementitious grout determines a yield surface or a transition region that separates the flow region and static region within narrow fractures. In simplified unidirectional flow within a

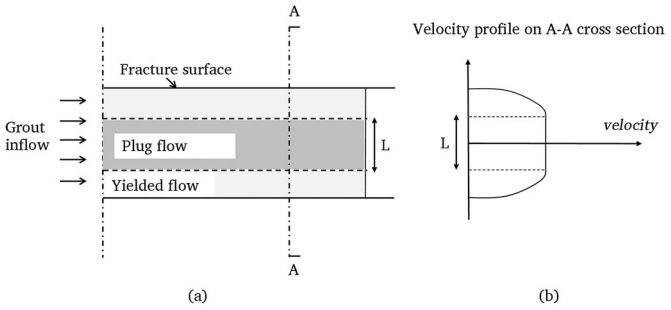

Fig. 4. Schematic of unidirectional grout flow between two parallel smooth fracture surfaces: (a) cross-section view; (b) idealized velocity profile, modified after (El Tani, 2012; Zou et al., 2020a).

smooth fracture (as sketched in Fig. 4a), a central solid plug region (where flow velocity remains constant) exists, along with a mobile flow layer (yielded region) adjacent to the fracture surfaces. The velocity drops sharply to zero under a no-slip boundary condition (in Fig. 4b). The parallel plate model simplifies a fracture as two smooth, parallel plates with constant separation, serving as a basis for more complex systems (Nazempour and Majdi, 2021). For a Bingham plastic grout flowing between two parallel plates of aperture 2 B and width W, under a pressure gradient ($-\frac{dp}{dx}$), Dai and Bird (1981) gave the volumetric flow rate (Q) by:

$$Q = -\frac{2WB^3}{3\mu_p}\frac{dp}{dx}\left(1+\frac{3}{2}\frac{\tau_0}{B}\frac{dp}{dx}-\frac{1}{2}\left(\frac{\tau_0}{B}\frac{dp}{dx}\right)^3\right) \tag{11}$$

The above equation applies to the radial flow configuration by replacing W with $2\pi r$ where r is the penetration radius. Zou et al. (2024) and their other work also gave the analytical solutions of flow rate-pressure gradient for Herschel-Bulkley fluid. However, disagreements exist regarding the exact analytical solutions, particularly concerning the gap-wise flux component and the nature of the plug flow region. Although different assumptions may predict a close flow rate-pressure relationship, the pressure distribution could be significantly different (Liu and Park, 2020).

Analytical solutions estimate grout penetration distance and grouting time in simplified scenarios and define the basic relationship between grout properties, injection pressure, and fracture aperture (Saeidi et al., 2013). Some analytical solutions address time-dependent grout rheology, typically applied to 1-D channels or radial plates (Mohajerani et al., 2017; Zhang et al., 2017). However, current analytical descriptions struggle with varying apertures (hydraulic jacking), fracture roughness, and flow transitions, limiting their direct applicability for understanding real-world grout behaviour and often necessitating numerical methods.

2.1.2. *Particulate view*

2.1.2.1. Origin of thixotropy. At the microscopic level, the origin of thixotropy in cement grout is dictated by the structure and strength of the network of cement particles. This network is primarily connected by various hydrate products, with calcium silicate hydrates (C–S–H) are believed to be the largest contribution (Roussel et al., 2012). Simplifying the granular materials in the grout as smooth round particles (in Fig. 5), grout particles can be categorised as: 1) dispersed particles with weak interparticle interactions, or 2) connected particles that aggregate into a rigid network. Most particles are fully dispersed initially. Without hydrodynamic forces, remote interactions such as the Van der Waals force, electrostatic forces (repulsive or attractive), Brownian motion, and steric hindrance (often due to polymer additives) control the movement of particles (Zang et al., 2024). Shortly after coming to rest (possibly in less than 1 s, depending on particle properties), cement hydration forms adhesive products that bond dispersed particles together, thereby increasing strength. Applied hydrodynamic forces (stirring, flow) can dismantle this network, which accounts for the grout's flowability and strength. The dispersed state (near the injection hole or under high flow) and bonded states (further from the injection point or under low flow) can coexist within fractures.

The cement grout's thixotropy is more complex than a simple continuum rheological model can fully capture due to its particulate nature. Roussel et al. (2019) used an oscillatory shear protocol to probe the viscoelastic properties of fresh cement paste for studying hydration and stiffening behaviour. Similar protocol was applied by Zang et al. (2024) to establish the macro-micro relationship of cement grout's thixotropy. Fig. 6 illustrates the macroscopic thixotropic behaviour of cement grout by presenting how shear stress evolves with strain. It demonstrates the good reversibility of early hydrate bonds which is attributed to the breakage of interparticle bonds, predominantly formed by C-S-H, under shear force and their subsequent reformation during resting periods. However, these defined phases are indirectly speculative results drawn from macroscopic observations. Fresh cement-based grout undergoes rapid transition from fluid-like state to a soft solid, and the evolution of micro-behaviour remains challenging to be quantified from sample to sample.

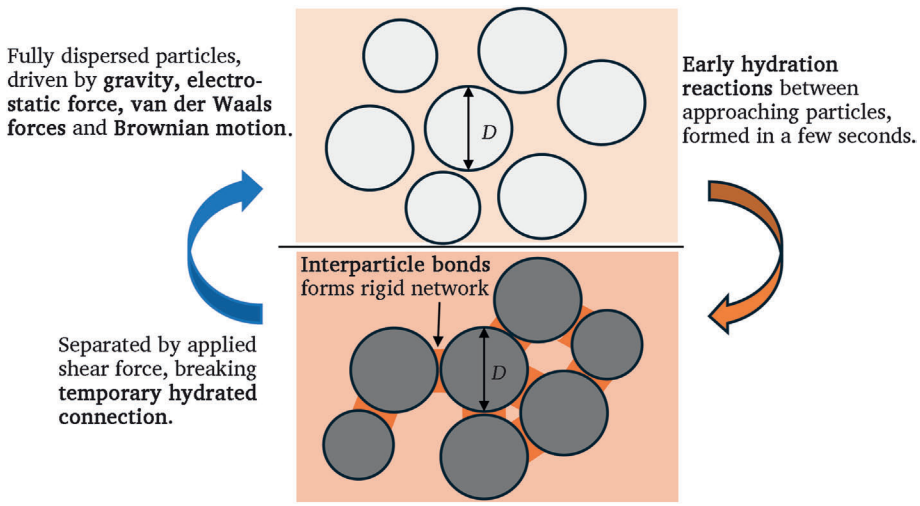

Fig. 5. Schematic description of the formation of cement network in grout, D is the diameter of the grout particle, modified after (Zang et al., 2024).

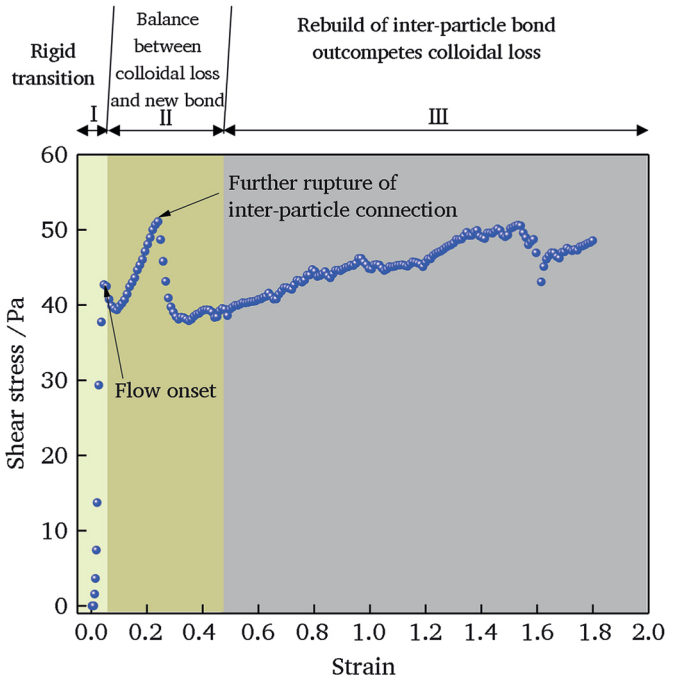

Fig. 6. Macroscopic representation of micro-evolution of interparticle bonds in a constant shear test (Zang et al., 2024).

2.1.2.2. Filtration and plug-building. For grout to fill rock voids effectively, particle size must be compatible with the fracture aperture, especially for fine joints. Barton and Quadros (2019) significantly contributed to the understanding of grout particle size compatibility. Their work highlights that grout particles can be too large to effectively penetrate very narrow fractures, leading to incomplete filling. An early rule-of-thumb found by Bhasin et al. (2002) suggests that, for fully dispersed grout (adding additives and using high-speed mixers), the minimum aperture should be $>$ 4 times the maximum particle size (or d95 size). However, Draganovic and Stille (2014) found that pressure filtration could invalidate this empirical rule. As illustrated in Fig. 7a, when grout encounters a narrowing or constriction where the aperture is smaller than a critical size, these particles cannot pass freely. The carrier fluid can continue flowing, but it loses solid particles relative to the original suspension (Lavrov, 2023). Pressure filtration can greatly reduce grout penetrability, especially at the intersection of the borehole and rock fractures. Fig. 7b illustrates plug formation near the entrance of a rock fracture; the filtered plug acts as a barrier, increasing flow resistance and potentially completely blocking further penetration into narrower parts of the fracture networks (Lu et al., 2020). It is recommended that the ratio of the minimum fracture aperture to the d95 particle size should be greater than 8 to reduce the likelihood of pressure filtration (Brantberger et al., 2000). The grout particle size distribution, solid/water ratio and grouting pressure also influence pressure filtration. Grouts with coarser particles or a wider range of particle sizes are more prone to filtration (Eriksson, 2002). The fluid phase in dilute grout can more easily break the filter cake. The blockage criteria mentioned above assume only physical clogging caused by dispersed grout particles. In practice, it is often necessary to apply additives to disperse grout particles in practice (Azadi et al., 2017).

2.2. Diffusion in fracture networks

The theoretical understanding of grout diffusion in complex fracture networks is largely established upon simplified single-fracture diffusion theories. Single-fracture theory defines the relationship between pressure, flow rate, fracture geometry, and grout properties for an isolated, simplified flow path. When considering fracture networks, the

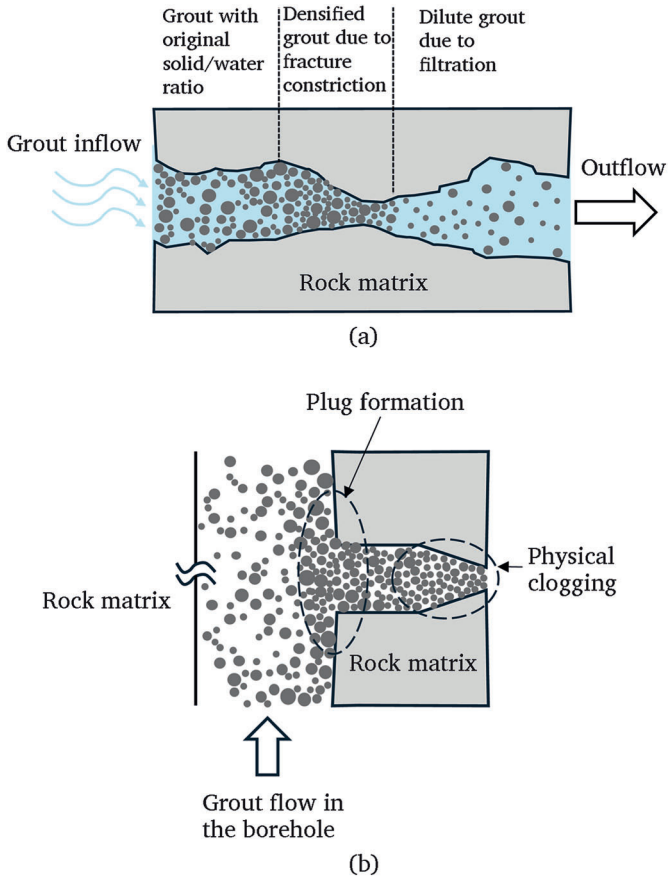

Fig. 7. Particulate description of granular grout mix flowing in rock fractures: (a) granular particles and water mix flowing in a rough fracture; (b) plug formation near the entrance of a rock fracture, modified after (Eklund and Stille, 2008; Wang et al., 2021).

conceptual approach is often to apply these single-fracture principles to each individual fracture element within the network; however, the integration of single-fracture diffusion into fracture network remains challenging due to the inherent complexity of natural rock masses (Zhang et al., 2017). Barton and Quadros (2019) discussed the use of a single hydraulic smooth aperture to represent the connectivity of physical fracture networks. This approximation is a compromise when dealing with fractured rock masses and provides basic inputs with parameter scoping in rock grouting design. Natural rock fractures exhibit significant roughness, tortuosity, and variable aperture distributions. The hydraulic aperture often differs significantly from the mechanical aperture. Ratios of physical to hydraulic aperture of 1.2–3 times are commonly reported (Saeidi et al., 2013).

Grout flow in a network is governed by the complex interconnectedness of individual fractures. Single-fracture theories do not account for branching, merging, dead-end fractures, or the flow partitioning at intersections (Lavrov, 2023). Rafi and Stille (2021) found that when grout flows into a junction or bifurcation within a fracture network, it experiences a significant pressure drop. The pressure decreases can also differ depending on the specific angles of the tributary fractures, and larger grouting pressures is recommended to effectively fill the network. routing pressure can induce deformation of fractures, which in turn affects grout flow in fracture networks (Zhu et al., 2019). Jiang et al. (2018) observed that grout diffusion at fracture intersections often exhibits a non-uniform spread shape. Moreover, the fracture-fracture interaction, particularly the position of pre-existing fractures and the grouting hole directly affect the splitting direction of fractures (Gothäll and Stille, 2010).

2.3. Stop criteria

Grout stop criteria in rock fracture grouting define when grout injection should cease. Some existing stop criteria are summarized in Table 1. The most common stop criteria rely on reaching limits within the grouting process itself, such as maximum grouting pressure (Rafi and Stille, 2014), maximum grouting volume (grout take), or a low grout flow rate (refusal) (El Tani and Lopez-Molina, 2020; Rafi and Stille, 2015). Grout Intensity Number (GIN) criterion combines the effects of both pressure and volume, defined as the product of pressure and volume (Al Kuisi et al., 2005; Brantberger et al., 2000). A specific GIN target value corresponds to an acceptable level of fracture dilation and grout spread. However, the relationship between energy and rock mechanics can be unclear, potentially leading to overestimation of grouting parameters (Fan et al., 2023). The GIN approach is theoretically attractive but can be difficult to implement. Similar to the maximum volume criterion, Aperture Controlled Grouting (ACG) limits the injected grout volume based on the available void space within interconnected fractures (Carter et al., 2012; Fan et al., 2023). Grout rheology is then adjusted to achieve pressure build-up for refusal at the required grout volume. These methods are often empirical, drawing on experience from previous projects, and limiting the energy input into the rock mass. Such simple limits do not guarantee a specific penetration distance and can be influenced by grout properties and fracture fillings (Yaghoobi Rafi, 2014). Alternatively, the low grout flow rate (refusal) criterion halts grouting when the flow rate into the fracture falls below a critical value (El Tani, 2012). This implies that the resistance to grout injection has become high, suggesting fractures are filled or the grout cannot penetrate further under the applied pressure. In small aperture fractures, this criterion can be particularly inefficient. The North American refusal criterion (NARC) is a typical example within this category.

In contrast to these empirical or process-based criteria, Rafi and Stille (2021) advanced the concept of stopping grouting based on achieved grout penetration distance and deformation limits. Their work led to the proposal of Deformation Limiting Curves (DLC), which aims to define acceptable limits for both grout spread distance and fracture deformation (jacking). This approach seeks to enable beneficial jacking (improving penetrability) without causing detrimental over-dilation or grout waste (Yaghoobi Rafi, 2014). These theoretically based criteria are generally preferred for optimising grouting efficiency compared to purely empirical limits. They also noted the use of grouting time as a stop criterion, either as a primary limit or in conjunction with other criteria. These methods require analytical solutions to estimate the grout spread in real-time or based on pre-calculated relationships, and are considered more theoretically sound for avoiding inadequate or uneconomical grouting compared to volume or flow-based criteria (Kobayashi and Stille, 2007). A representative example is the Real-Time Grouting Control (RTGC) method proposed by Gustafson et al. (2013)

Table 1
Comparison of different stop criteria for rock fracture grouting.

Criterion	Description	Underlying assumption	Limitations	References
Maximum grouting pressure	Stop grouting when a predefined maximum pressure is reached.	Exceeding this pressure could cause damage (e.g., hydraulic fracturing, uplift, uncontrolled spread).	Does not account for the actual extent of grout penetration or fracture filling.	Rafi and Stille (2014)
Maximum grouting Volume (grout Take)	Stop grouting when a predefined volume of grout has been injected.	Injecting this volume will adequately fill the fractures.	(a) May overfill large fractures leaving finer ones untreated (or vice versa); (b) potentially inefficient or uneconomical without knowing the specific fracture geometry or connectivity.	Kobayashi and Stille (2007)
Low grout flow rate (Refusal)	Stop grouting when the flow rate falls below a critical minimum value.	High resistance indicates fractures are filled or grout cannot penetrate further at the applied pressure.	(a) Does not guarantee a specific penetration distance; (b) influenced by grout properties and fracture characteristics; (c) can be inefficient, especially in fractures with small apertures.	(Ann Emmelin et al., 2007; El Tani, 2012; El Tani and Lopez-Molina, 2020; Rafi and Stille, 2015; Yaghoobi Rafi, 2014)
Aperture controlled grouting (ACG)	Stop based on injecting a volume calculated from estimated interconnected void space (fracture aperture); adjust grout properties to achieve refusal at this volume.	Filling the estimated void volume achieves effective sealing. (Often uses DFN modelling).	Relies heavily on accurate estimation of interconnected void volume and aperture, similar to the maximum volume criterion.	(Carter et al., 2012; Fan et al., 2023)
Grout intensity number (GIN)	Stop grouting when the product of injection pressure and injected volume reaches a target value.	Combines pressure and volume effects; intended to limit energy input to control rock mass deformation and grout spread.	(a) Relationship between GIN value (energy) and rock mechanics response can be unclear; (b) potential overestimation of grout spread; (c) difficult to implement effectively; (d) actual spread distance is unknown at the stopping point.	(Al Kuisi et al., 2005; Brantberger et al., 2000; Fan et al., 2023)
Achieved grout penetration distance	Stop grouting when grout has theoretically penetrated a desired distance (often estimated using analytical solutions, e.g., in RTGC methods).	Achieving the target penetration distance effectively seals water pathways or strengthens the rock mass as intended.	Relies entirely on the accuracy of the underlying analytical models and the quality of input parameters (e.g., aperture, grout rheology).	(Gustafson et al., 2013; Kobayashi and Stille, 2007; Shamu et al., 2021)
Deformation limiting curves (DLC)	Stop grouting when the required grout spread is achieved without exceeding a defined limit on fracture deformation (jacking).	Controls fracture deformation (beneficial jacking) within acceptable limits to avoid rock mass damage or grout waste.	Requires reliable deformation monitoring and accurately defined deformation limits for the specific site conditions.	Rafi and Stille (2021)
Grouting time	Stop grouting after a predefined duration of injection.	Assumes sufficient time under given conditions allows grout to penetrate the necessary distance (often based on experience or simple theoretical relations).	(a) A fixed time may not be optimal; (b) actual penetration depends significantly on aperture, grout properties, and injection pressure, which can vary.	(Ann Emmelin et al., 2007; Rafi and Stille, 2021)

using analytical solutions to estimate real-time penetration. It informs stop criteria based on achieving minimum and maximum penetration distances in different fracture apertures.

The choice of the most appropriate stop criterion depends on the specific project objectives, geological conditions, grout properties, and available monitoring tools. Theoretically based criteria considering grout penetration and fracture deformation are generally preferred for optimising grouting efficiency (Kobayashi and Stille, 2007). However, empirical criteria remain widely used due to their simplicity and reliance on practical experience. Increasingly, integrated approaches combining theoretical understanding with real-time monitoring and adjustments are being advocated for improved grouting outcomes.

2.4. Challenges and prospects

Despite improved understanding, gaps between theoretical grouting models and their practical application hinder theory testing and refinement. A major challenge is establishing a robust quantitative link between particulate descriptions (e.g., filtration, clogging) and continuum parameters like yield stress and viscosity. Zang et al. (2024) used dimensionless analysis to assume initial electrostatic forces dominate interparticle interactions between separate cement particles. Their work illustrates how calcium silicate hydrates (C-S-H) form reversible bonds as particles approach (Fig. 8). The C-S-H bonds are not as strong as permanent bonds and can be broken under applied force, leading to a cycle of reversible temporary interparticle bonding in cementitious grout. This theory matches macroscopic observations from laboratory rheometric tests (Roussel et al., 2012). Further establishment of particulate theory could help connect discrete particle behaviour statistically with the continuum description of non-Newtonian fluids. However, an unsolved issue is that non-Newtonian models typically use yield stress for flow initiation and do not explicitly explain potential flow stoppage due to particle blockage in narrow fractures.

Most analytical expressions use critical thresholds for grout flow onset; different thresholds may cause significant flow rate–pressure mismatches. These thresholds cannot account for the transition between yielded and unyielded states (Zang et al., 2024). Some also use lubrication theory, which essentially neglects inertia and gap-wise vertical grout flow across the fracture. The applicability of these simplifications to non-Newtonian grout flow in rough fractures is uncertain. More work is needed to investigate lubrication theory validity and to develop analytical models incorporating roughness, especially for non-Newtonian flow at higher flow rates.

Theoretically describing the mixed flow of non-Newtonian grout and water is difficult. Two-phase flow, where grout displaces water, critically impacts grout front pressure and can slow penetration (Lavrov, 2023). Incorporating this into analytical solutions is challenging due to unclear mechanisms governing different flow regimes. The interplay between these two-phase effects and grout hardening time further complicates analysis. Grout injection pressure can widen fractures, altering flow paths and penetration distance (Gothäll and Stille, 2010). The coupled hydro-mechanical (HM) behaviour cannot be simplified solely as aperture expansion. Using pressure exceeding in-situ stresses for better penetrability risks hydraulic jacking and grout waste if stop criteria are inappropriate (Zou et al., 2024). Balancing penetrability benefits against dilation risks needs further investigation.

3. Developments in experiments

Laboratory tests enable controlled observation of grout diffusion through artificial or simulated fractures. Historically, investigations relied on simplified representations like parallel plates. However, there has been a notable shift towards more sophisticated experimental approaches aimed at replicating real-world fracture networks complexities and flow conditions. This section focuses on new laboratory approaches for studying grout flow in rock fractures, excluding studies solely on grout material rheological properties. For information on the measurement of grout rheological properties, interested readers may refer to the literature (Dinkgreve et al., 2016; Dzuy and Boger, 1983; Rahman et al., 2017).

3.1. Laboratory-scale observations

3.1.1. Parallel plate tests

Most experimental models for grout propagation have historically

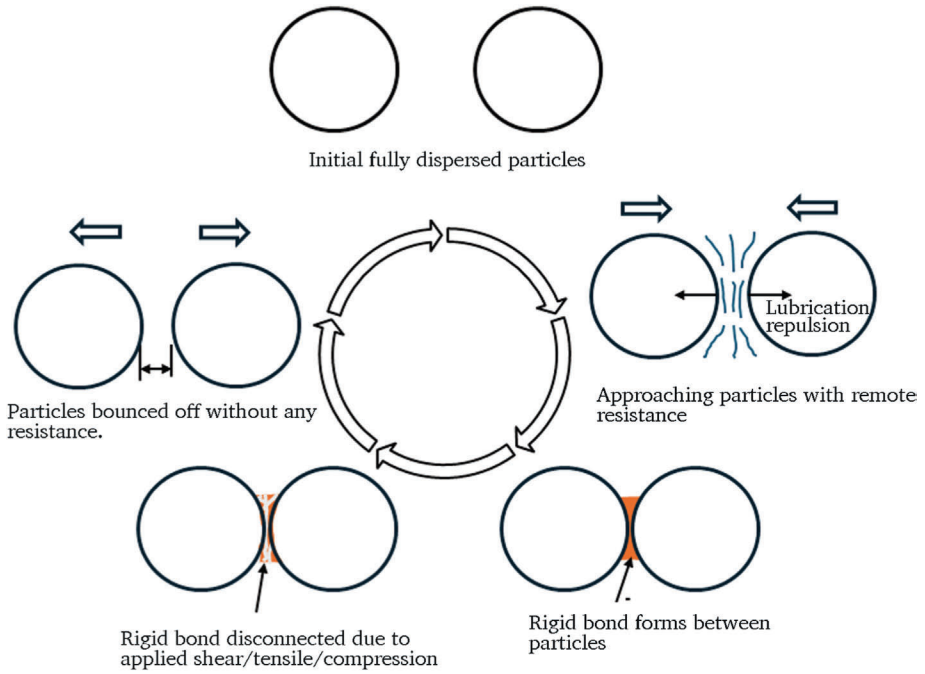

Fig. 8. Circulation of interparticle bonds between an interacting pair of cement spheres, modified after (Zang et al., 2024).

utilised smooth, rigid parallel plates, often with a constant aperture, to study fundamental grout flow characteristics. Mohammed et al. (2015) used a fracture device comprising two stiff plexiglass discs with apertures ranging from 100 to 500 μm to demonstrate that effective cement grout penetration increased with aperture. They also studied the impact of static and oscillatory pressures, suggesting that oscillatory pressure could improve penetrability by reducing grout viscosity. Funehag and Thörn (2018) verified the radial Bingham flow of cementitious grout using an acrylic glass fracture model, filming grout spread over time and comparing it to analytical solutions for smooth parallel plates. Lee et al. (2019) employed planar acrylic plates with variable separation distances to measure grout penetration length under different injection rates and apertures, verifying their numerical estimations. Shamu et al. (2020) measured radial velocity profiles of Carbopol using the pulsed ultrasound velocimetry within a radial flow model, their results agreed well with analytical solution and highlighted the plug-flow region and slip effects. Han et al. (2020) utilised smooth rectangular plexiglass discs to study the influence of periodic pressure adjustments on grouting efficiency, concluding that phased reduced pressure significantly improved efficiency.

While parallel plate experiments have been indispensable for studying fundamental principles of grout flow due to their controlled nature, their simplified representation of reality necessitates a cautious interpretation of results. Duan et al. (2025) revealed that smooth parallel-plate models can overestimate the grout filling rate by about 30% and significantly underestimate grout flow. Their work show that ignoring properties like wall-slip can lead to substantial inaccuracies, potentially overestimating grout travel by up to 50%. Many early parallel plate models simplified grout flow as a single-phase process. However, grout displacement of groundwater is a two-phase process that critically impacts pressure distribution and grout penetration in water-saturated environments. Zhu et al. (2020) used a fracture grouting simulation test platform to observe grout diffusion patterns under water scouring. They found an asymmetric ellipse diffusion pattern when subjected to flowing water (see Fig. 9), suggesting that the flowing water offers resistance to the grout's propagation.

3.1.2. Grouting rough fractures

3.1.2.1. Roughness characterization. Laboratory techniques increasingly aim to realistically simulate field conditions, moving beyond early simplified fracture models. Various methods exist for characterising fracture roughness in laboratory physical models, as illustrated in Fig. 10. Some use artificial fractures with controlled geometries, such as saw-tooth patterns, laser-cut acrylic, casts made from cement based on Barton's standard roughness profiles, or 3D prints based on statistical data. Alternatively, some studies characterize real or artificial surfaces using laser scanning to capture detailed topography for analysis or model creation (Singh et al., 2015; Zou et al., 2024), or use image processing of standard profiles (Wang et al., 2020). The method chosen often depends on whether the study focuses on grout penetration, fluid flow, or mechanical behaviour.

Converting rough fractures to an equivalent smooth hydraulic aperture is common for grouting design. Empirical relationships allow this estimation without direct field measurement of roughness. A well-known method uses the Joint Roughness Coefficient (JRC) to relate the physical aperture (E) and hydraulic aperture (e) (Barton et al., 2023; Widmann, 1996). The hydraulic aperture is related to the physical aperture E and JRC through Barton's work, via the relation $e = \frac{\mathrm{JRC}^{2.5}}{(E/e)^2}(\mu\mathrm{m})$. Zimmerman and Bodvarsson (1996) incorporated the effects of aperture variability and contact area, considering an arithmetic mean aperture e_{mean} and standard deviation δ_e of the aperture. They proposed a relationship for the hydraulic aperture $e^3 = {e_{\mathrm{mean}}}^3\left(1 - \frac{1.5{\delta_e}^2}{{e_{\mathrm{mean}}}^2}\right)(1 - 2c)$, where c is the fraction of contact area. This suggests that the variability in aperture and contact area reduce the effective hydraulic aperture compared to the arithmetic mean. There are also site-specific empirical coefficients, such as those relating to void filling aperture and implicitly accounting for roughness and flow channelization (Carter et al., 2012). These conversions have simplified calculations, but they rely heavily on empirical data and subjective comparisons with standard profiles (such as JRC estimation).

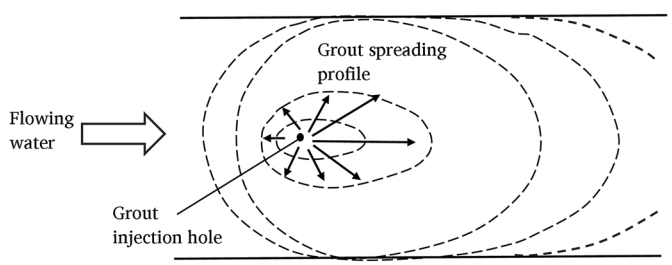

Fig. 9. Schematic description of asymmetric ellipse diffusion pattern of grout under water scouring, modified after (Zhu et al., 2020).

3.1.2.2. Impact of fracture roughness. Laboratory tests consistently demonstrate that fracture roughness significantly changes grout flow compared to predictions for smooth fractures. Wang et al. (2021) used a large-scale 3D-printed rough fracture models to simulate grouting to study grout flow patterns and concentration distribution. Their results show that fracture roughness causes uneven grout front advancement due to preferential flow paths. This reduces the effective transmissivity for non-Newtonian fluids, suggesting less flow for a given pressure gradient and slower spread rates (Ding et al., 2020; Yang et al., 2020; Zou et al., 2021). The relationship between fracture roughness and grout sealing efficiency remains relatively unexplored. Trinchero et al. (2024) found that a hydraulic aperture equal to 1/5 of the mechanical aperture of a natural rough fracture provided a reasonable approximation of experimental flow rates using the cubic law, meaning the hydraulic aperture is typically only a few tenths of the mechanical aperture in crystalline rocks. Chen et al. (2024) observed a T-shaped grout distribution profile was observed in rough fractures with a JRC of 18–20, which was attributed to gradual grout deposition and a significant flow rate drop. Roughness also increases grout pressure loss along the flow path and can cause grout thinning (concentration decrease) due to filtration effects. Fig. 11 illustrates how fracture roughness hinders penetration and changes flow direction near the fracture surface. The grout collected at the outlet consists mainly of the middle part with a lower solid ratio, accounting for shear-thinning effects in rough fractures.

Although roughness affects pressure build-up and flow rates, current grout injection stop criteria often do not explicitly account for it. Some theoretical approaches attempt to incorporate factors implicitly related to roughness into stop criteria, such as the Grouting Intensity Number (GIN) method, which utilises pressure and volume as key parameters to determine when to stop injection. The effect of roughness is not explicitly defined in the GIN, but the change in pressure and flow rate are influenced by fracture characteristics (Yaghoobi Rafi, 2014). Li et al. (2024) developed and validated a theoretical model that considers the combined effects of fracture roughness, aperture, and grouting pressure on grout diffusion. Their findings suggested that while roughness and aperture have a relatively minor impact on grout pressure distribution, grouting pressure itself exerts a significant influence. However, the complex surface texture of rough fractures introduces variability in these parameters, making the application of standard stop criteria less straightforward. Du et al. (2021) demonstrated that in cement-grouted fractures with flowing water, fracture roughness represented by its tortuosity shows a distant-dependent effect. This is attributed to increased energy dissipation and particle deposition in more tortuous (rougher) flow paths closer to the grout injection point.

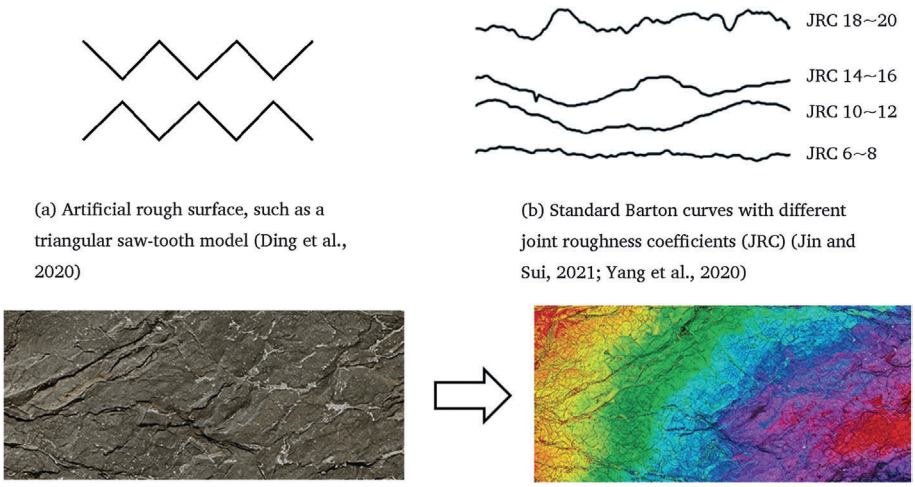

(a) Artificial rough surface, such as a triangular saw-tooth model (Ding et al., 2020)

(b) Standard Barton curves with different joint roughness coefficients (JRC) (Jin and Sui, 2021; Yang et al., 2020)

(c) Digitized surfaces obtained from high-resolution optical scanning (Wang et al., 2021; Zou et al., 2024)

Fig. 10. Different approaches for characterising fracture roughness for laboratory tests on rock fracture grouting.

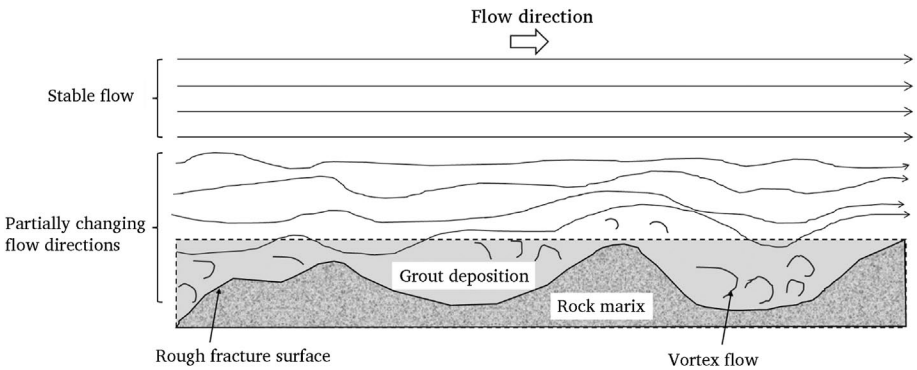

Fig. 11. Evolution of grout deposition in rough fractures (upper surface removed for visualisation), modified after (Chen et al., 2024).

3.2. Advancements in monitoring and measurement approaches

Traditional laboratory tests provide direct macroscopic observations of essential flow parameters. For instance, Zhang et al. (2025) used two parallel transparent acrylic glass plates to observe viscous fingering of cement grout as it diffused under flowing water after injection ceased. Draganovic and Stille (2014) employed four pressure sensors along a 4 m slot with a 75 mm gap to monitor the pressure gradient, indicating filtration and plug-building during grout flow. While these methods offer fundamental information, they provide limited insight into detailed flow paths, velocity variations, or grout distribution heterogeneity within the fracture. To address this, Rahman et al. (2015) utilised advanced in-line rheological techniques, specifically ultrasound velocity profiling coupled with pressure measurements, to visualize and measure actual velocity profiles. This spatially dynamic data revealed that grout distribution and heterogeneity within a fracture can vary significantly, even with a consistent total injected volume. This demonstrates that relying solely on total volume as a stop criterion or measure of sealing efficiency can be misleading, as seal quality depends on intricate flow patterns and how effectively grout fills void spaces.

Most recently, advanced techniques have begun to offer a more detailed, dynamic understanding of grout flow in laboratory-scale fractures. Acoustic emission (AE) monitoring uses sensors to detect micro-fracturing events triggered by grout injection (Liu et al., 2020b). Analyzing AE data (such as counts over time and 3D source positioning) provides insights into fracture initiation, filling, and propagation stages. Lee et al. (2021) used electrical resistivity (ER) measurements to track grout penetration non-destructively by monitoring changes in electrical resistance within fractures during injection, exploiting the electrical property difference between grout and existing fluids. Weng et al. (2022) employed low-field nuclear magnetic resonance (LF-NMR) as a non-destructive method for evaluating grouting in fractured samples. By tracking NMR signals over time (intensity relates to mobile water/-hydrogen in grout), researchers can monitor grout filling speed, post-grouting pore structure changes, filling efficiency, and how external conditions affect the process.

These non-invasive methods (AE, ER, NMR) are valuable for tracking grout spatially and temporally where visual access is impossible. However, their efficiency depends on signal strength, influenced by monitoring distance, material properties, heterogeneity, and resolution (Ramskill et al., 2018). For post-experiment analysis, Liu et al. (2020b) used dye tracers to visually reveal grout pathways. Bo et al. (2024) track tracer particles by Particle Image Velocimetry (PIV) to map grout velocity fields, aiding model validation.

To avoid the costly on-site drilling process, Zang et al. (2025) developed a novel inverse model with surface magnetic measurements at different heights to estimate grout sheet depth, angle, and spread (see Fig. 12). This method is reported to be applicable for observation height up to five times the grout sheet length. This magnetic approach is still developing and needs more field testing. All these methods require a clear difference in physical properties between the grout and rock, and sufficient expertise in geophysics and geological conditions. If the grout's physical properties are too similar to the host materials, the efficiency can be severely compromised. Their ability to provide fine details (spatial resolution) is limited, making precise imaging of grout in fine rock joints challenging. Nonetheless, compared traditional intrusive

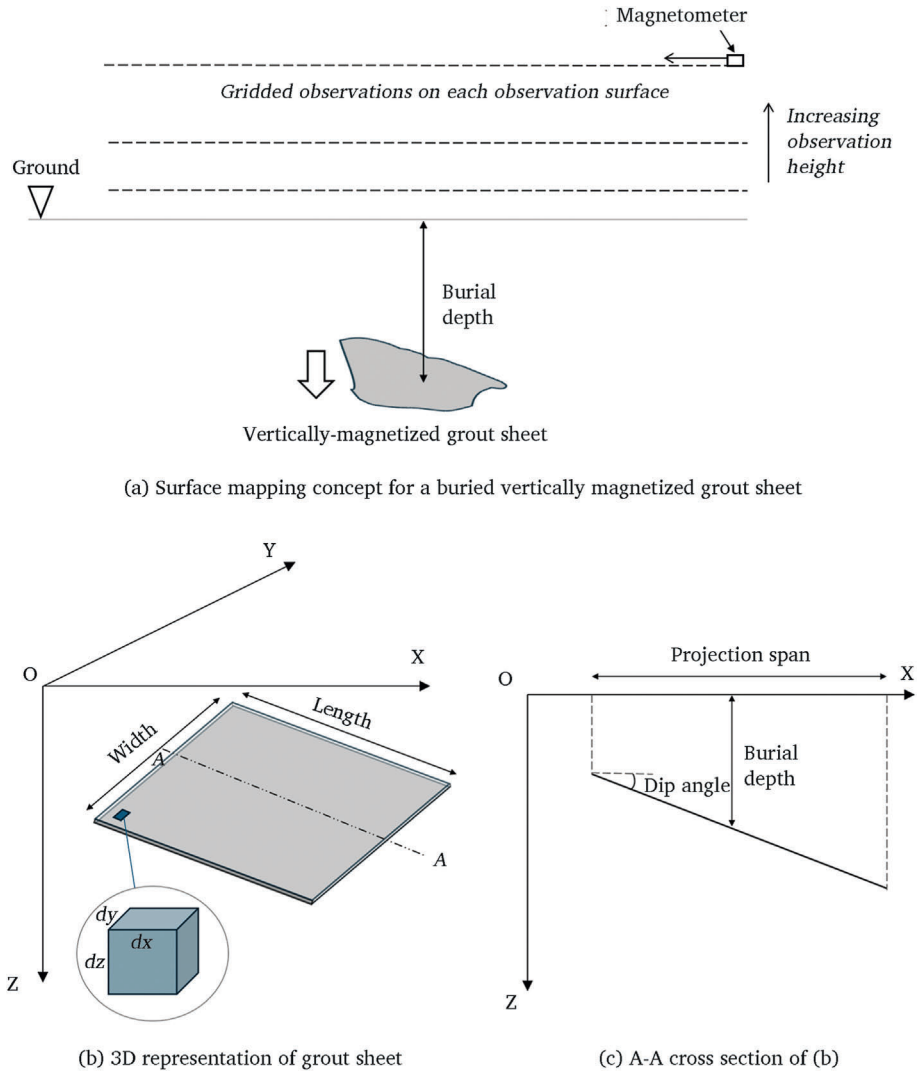

Fig. 12. Schematic illustration of magnetic detection of a grout sheet, modified after (Zang et al., 2025).

testing, these non-destructive techniques offer potentially cost-effective ways to evaluate grouting over large areas.

3.3. Developments of testing apparatus

Advanced laboratory tests for rock fracture grouting, which are often used in combination, aim to overcome the limitations of traditional macroscopic measurements. Novel setups frequently incorporate real-time, computer-based monitoring to continuously capture dynamic grout flow and pressure data (Fransson et al., 2007; Jin and Sui, 2021; Nejad Ghafar et al., 2017; Zou et al., 2024). Beyond standard parameters, measuring properties like the pH value at the grout front also offers a cost-efficient way to detect grout arrival (Henderson et al., 2008).

Ghafar et al. (2017b) developed the Varying Aperture Long Slot apparatus featuring a 4 m artificial fracture with apertures varying down to 10 μm (in Fig. 13). It enables the study of how aperture variations affect grout penetrability and filtration, monitoring injected weight and pressure (up to 1500 kPa) along the slot under static and dynamic conditions. This contrasts with earlier penetrability meters developed by Eriksson et al. (2004), which used mesh filters better suited for porous media. This is because the mesh structure in the penetrability meter supports plug formation from four sides, whereas a slot only provides support from two sides (Nejad Ghafar et al., 2017), especially considering that the length of the constriction zone in the penetrability meter (at most 100 μm) can be much shorter than in real rock fractures.

Ghafar et al. (2016) explored varying boundary conditions, such as dynamic or pulsed pressure, to enhance grout penetration by controlling filtration. Compared to steady pressure, dynamic pressure with low-frequency pulses can reduce particle blockage and weaken dominant flow channels, which is confirmed in controlled constriction tests (Nejad Ghafar et al., 2015). However, conflicting results exist for high-frequency oscillations, which might cause heating, accelerate hydration, increase viscosity, and thus potentially reduce penetration (Meng, 2021). The choice between dynamic and constant pressure requires careful consideration.

Zhu et al. (2020) developed a large-scale quasi-three-dimensional fracture replica measuring 4000 mm long and 2000 mm wide (in Fig. 14) with monitoring pressure sensors along the penetration path. This enables the study of cement-sodium silicate (C-S) grout diffusion and sealing mechanisms under flowing water conditions, and it represents real-world fracture geometries compared to simplified two-dimensional models often used in analytical and numerical studies.

To study particle-scale flow mechanisms, Lu et al. (2020) developed microscopic visualisation systems using long-working-distance microscopy. These allow visual capture of filter cake formation at the fracture inlet, revealing how different particle sizes contribute under varying apertures and enabling observation of particle-wall interactions at this microscale. Quantitative image analysis showed filter cakes grow

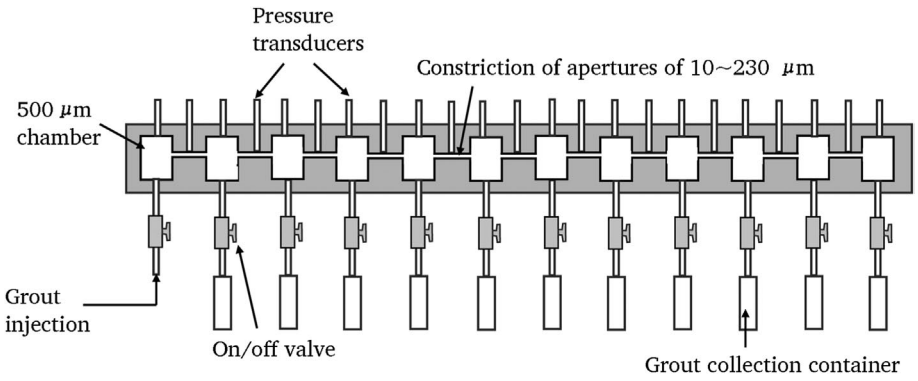

Fig. 13. Schematic depiction of Varying Aperture Long Slot apparatus, modified after (Ghafar et al., 2017b).

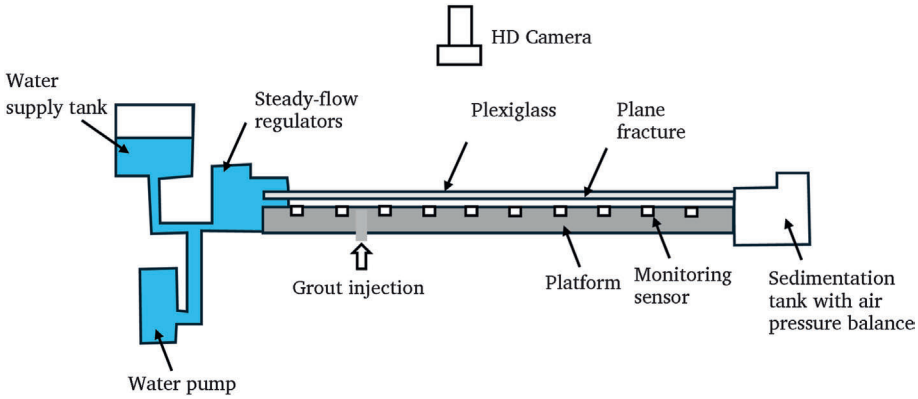

Fig. 14. Schematic plot of water-grout two-phase grouting platform, modified after (Zhu et al., 2020).

rapidly, with formation starting later in wider apertures.

3.4. Limitations

Current laboratory rock fracture grouting tests face significant hurdles in replicating in-situ conditions. A major challenge is the inability of simulated rock materials to fully represent the heterogeneity and complexities of natural fractures, which exhibit rough surfaces, variable apertures, and often contain infill materials. Intricate, interconnected 3D fracture networks are typically simplified to single fractures or regularly distributed networks in experiments, potentially overlooking crucial interactions between multiple discontinuities.

Another significant limitation is accurately simulating hydro-mechanical (HM) coupling at laboratory scale. In-situ rock fracture boundary conditions differ vastly from laboratory idealizations, potentially leading to unrealistic grout movement. Achieving the equivalent stress states mimicking the high confining pressures in deep underground scenarios is difficult. Factors such as groundwater flow and pressure, temperature variations, and the scale of the rock mass are difficult to accurately simulate. Consequently, no single experimental setup can perfectly capture all facets of in-situ conditions. Ideally, experimental setups should account for the mechanical behaviour of the surrounding rock mass and the influence of in-situ stresses. This could involve applying confining pressure to rock samples containing fractures during grouting experiments to simulate depth effects and study hydro-mechanical coupling.

Many experimental studies focus on the individual influence of single or a few grouting parameters, lacking a comprehensive analysis of the combined effects of multiple parameters on grout penetration. For example, the interaction between time-dependent grout properties and fracture roughness under flowing water might not be fully explored. The long-term performance and durability of grout seals in fractures under various conditions also require more extensive investigation.

While microscale visualisation offers invaluable insights into grout behaviour at a particle level, its small scale restricts the ability to extrapolate findings to the larger scales and complex geometries encountered in natural systems. Awareness of these typical limitations is necessary when choosing an experimental approach to investigate specific behaviour, including scaling effects, mismatches in temporal scales, and the challenges of replicating groundwater interactions. These highlight the ongoing need for innovative approaches to bridge the gap between simplified experimental observations and the practical applications of fracture grouting.

4. Advanced numerical modelling of grout flow in fracture networks

Numerical simulation offers a crucial advantage for investigating grout diffusion in complex fracture networks by providing dynamic, continuous solutions under intricate conditions, moving beyond broad assumptions inherent in purely theoretical research and physical experiments. This approach enables parametric studies unburdened by physical constraints of model size or measurement precision. Furthermore, numerical models overcome limitations posed by empirical relationships and simplified assumptions for variable aperture, roughness, and connectivity of natural fracture networks, providing scientific guidance for laboratory test designs.

4.1. Computational methodologies

4.1.1. Continuum matrix (CM)

Continuum matrix (CM) models treat fractured rock as a single continuous medium (Fig. 15a) using averaged properties instead of explicit fractures (Rutqvist and Stephansson, 2003). Fracture effects are

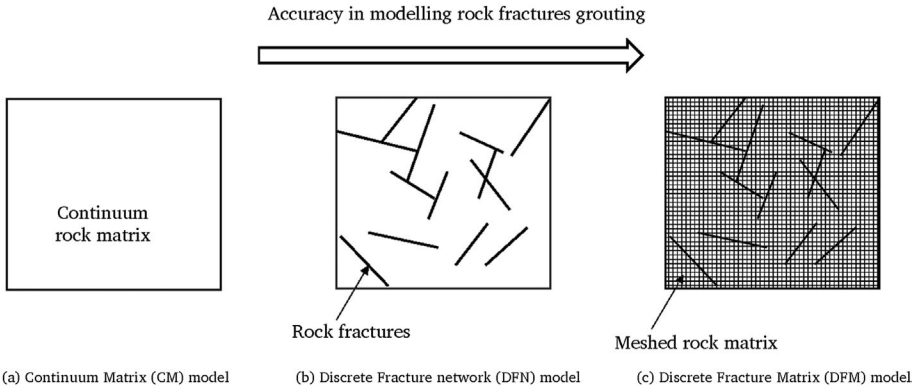

Fig. 15. Schematic illustration of different numerical approaches for simulating fracture networks.

incorporated by upscaling or homogenizing them into equivalent rock mass properties, often defining an effective permeability tensor to account for both the intact rock matrix and the discrete fractures contributing to the overall flow capacity (Viswanathan et al., 2022). Grout flow typically follows Darcy's law or its modifications, driven by pressure gradients and dependent on hydraulic conductivity and grout viscosity (Berre et al., 2019). Non-Newtonian grout behaviour can be included in the pressure-flow relationship. CMs are especially suitable for early project stages with relatively simple fracture systems and are less computationally demanding (Ma et al., 2025). However, the precise effect of individual fractures and their connectivity is completely lost during the upscaling process, particularly in highly heterogeneous rock.

4.1.2. Discrete fracture network (DFN) and discrete fracture matrix (DFM)

DFN and DFM models move beyond the averaged properties of continuum models by explicitly representing the fracture network. As shown in Fig. 15b, DFNs represent individual fractures as channels (one-dimensional pipes or two-dimensional lines) (Nazempour and Majdi, 2021) or planar polygons/discs in three dimensions (Lei et al., 2017) with defined geometry (orientation, size, position, aperture) (Eriksson, 2002). Mohajerani et al. (2017) developed an efficient algorithm for simulating grout propagation in 2D DFN and extended their methods to calculate grout permeability in 2D and 3D random fissure networks. Zou et al. (2019) extended the two-phase flow model for cement to 2D DFN systems and developed a new algorithm for tracking grout propagation interfaces by adding moving nodes in each fracture, which overcomes difficulties in resolving pressure and avoids extra iterations found in traditional methods. Xiao et al. (2019) developed a grouting program based on discontinuous deformation analysis to investigate the impact of 2D fracture distribution and connectivity on grout diffusion, while they simplified grout properties by considering them constant over time and neglecting crack roughness. By utilising a connectivity matrix to digitize topological structures, Liu et al. (2021) created a dynamic diffusion and migration algorithm for grout in 2D fracture networks, which significantly reduced computation time. They observed that when grout disperses into multiple branches within a fracture network, significant pressure drops and decreased flow velocities occur, with bifurcation angles heavily influencing pressure and flow distribution. DFNs offer a more realistic portrayal of heterogeneous fractured rock than continuum models, allowing the study of how individual fracture properties and network connectivity influence grout spread and sealing effectiveness (Kvartsberg, 2013; Liang et al., 2024). However, basic DFNs often assume an impermeable matrix, ignoring grout leak-off, potentially underestimating the grout take and pressure loss.

DFM models aim to include matrix interaction by embedding explicit fractures within a continuum matrix domain (Berre et al., 2019; Tong et al., 2022). As illustrated in Fig. 15c, grout flow is simulated in both fractures and the surrounding porous matrix (using Darcy-like equations or others). DFMs account for fluid exchange between fractures and matrix, better simulating grout leak-off into permeable rock and interaction with groundwater. Similar to DFN models, generating computational meshes conforming to both domains can be exceedingly challenging in DFM models. However, the use of DFN and DFMs, especially in 3D, can be computationally intensive, as more geological parameters require calibration and sampling due to inherent uncertainties in fracture location, size, orientation, and hydrological properties (Sun et al., 2023).

4.1.3. Hybrid methods

Hybrid methods combine the strengths of continuum and discrete approaches, offering a balance between detail and computational cost by selectively representing fractures. These approaches aim to leverage the strengths of individual methods while mitigating their limitations. In these models, large dominant fractures can be explicitly represented using methods like the finite element method (FEM), while the rest of the fracture network can be treated implicitly as a continuum with modified properties (Barton et al., 2023). The most common application of hybrid methods is modelling the hydro-mechanical coupled effect of grouting (Fransson et al., 2007). The combined finite-discrete element (FDEM) method is particularly suitable for complex continuous-discontinuous transition processes that model fracture initiation, propagation, and solid mass deformation, while grout flow is typically modeled based on a parallel-plate model (Sun et al., 2019). Liu and Sun (2019) extended the FDEM by incorporating the Bingham model to investigate the HM coupling effect on the grouting process. Yin et al. (2024) have integrated fluid flow solver frameworks into FDEM to simulate fluid flow in fractures and the coupled HM interactions during processes like hydraulic fracturing. Moreover, Liang et al. (2024) used numerical manifold method (NMM) to handle the deformation of both rock matrix and discrete fractures. Despite these advancements, these models neglect the time-dependent rheological characteristics of grout, such as the increase in viscosity and yield stress over time. This time-dependency can significantly affect the resistance to grout flow, thereby reducing the penetration rate and the final penetration distance (Yin et al., 2024).

4.1.4. Discrete grout and lattice Boltzmann method (LBM)

Grout suspensions can be modeled using discrete particles. This allows the study of particle migration, deposition, and potential fracture plugging influenced by fluid forces (drag) and interparticle contact forces. For example, CFD-DEM coupling models the fluid phase (using CFD) and solid aggregate particles (using the DEM) separately. Ren et al. (2022) employed a CFD-DEM coupling model to study the migration characteristics and restoration mechanism of grout containing aggregate in overburden fractures. Their model integrates the mechanical constitutive model of aggregate migration with the fluid flow, providing insights into aggregate transport and deposition characteristics. However, the fluid phase in this model still uses macroscopic rheological parameters that lack a direct connection to the mesoscopic behaviour of solid

particles. The Lattice Boltzmann method (LBM) operates at an intermediate (mesoscopic) scale, bridging micro and macro behaviour (Deng et al., 2018; Hu et al., 2022). It represents grout via fluid particle distributions on a discrete lattice, with macroscopic properties emerging from the statistical behaviour of these distributions as they evolve. Ortega and Vergara (2024) have investigated the reinforcement behaviour of fractured rocks using LBM, incorporating modifications to the relaxation parameter. This method can simulate sudden expansion and contraction, which are common geometric features in fractured rocks, providing insights into pressure distribution and energy losses. LBM handles complex geometries and can be adapted for multiphase flow (e.g., grout displacing water using Volume-of-Fluid techniques). However, LBM does not track individual grout grains explicitly, and its statistical nature can make representing complex cement grout rheology (thixotropy, hydration) challenging without sophisticated modifications or coupling.

4.2. Recent numerical insights

Some key findings regarding grout flow in rock fractures can be more readily drawn from numerical modelling than from theoretical or laboratory solutions. Significant advancements in the visualisation of grout spread in complex 3D fracture networks allow quantification of how factors such as fracture density, size distribution, orientation, and the number of intersections affect the overall grout penetration volume and rate (Tong et al., 2022; Zou et al., 2021). Zou et al. (2019) found that although more connected networks may offer more pathways for grout spread, they may also lead to more complex and potentially less predictable flow patterns. They also observed that uncorrelated heterogeneous apertures reduced propagation volume fraction and increased its variability, while correlation of aperture to fracture length notably increased the propagation rate and reduced variability.

Simulation of HM coupling can reveal the impact of fracture dilation (or jacking) occurring due to the pressure exerted by the injected grout on fracture surfaces. Rafi and Stille (2015) extensively investigated the basic mechanism of elastic jacking and its impact on grout spread. Their studies show that fracture dilation can lead to increased penetration distances compared to scenarios where the aperture is assumed constant. Conversely, if the rock mass is stiff or in-situ stresses are high, fracture dilation might be limited. Zhou et al. (2018) used cohesive finite elements coupling stress-seepage-damage fields to allow for fluid exchange between the porous medium and fractures, and they found a significantly lower pore pressure near the fracture tip when considering the effect of fluid. Considering stress interaction between neighbouring fractures, Sun et al. (2019) found that injection into one can influence the stress state and aperture of adjacent fractures, affecting grout flow there and highlighting the limitations of isolating single fractures in modelling.

CFD approaches in 3D fracture networks have enabled the simulation of non-Newtonian grout flow. These models can account for the yield stress and viscosity of the grout, showing how these rheological properties influence the grout's penetrability in fractures of different apertures and the resulting pressure distribution in the fracture network (Gao et al., 2024; Zou et al., 2021). Zou et al. (2020b) demonstrated that increased yield stress, consistency index, and flow index in models like the yield-power-law model can lead to a reduction in propagation rate and the overall volume of the fracture network filled by grout.

Computational modelling offers valuable insights into grout flow mechanisms at different scales. At the single fracture scale, models like the FEM and CFD are frequently employed to analyse the impact of fracture geometry, including aperture variation and roughness, on grout flow patterns and penetration (Cui et al., 2021; Ding et al., 2020). A single fracture provides a fundamental starting point for studying single-phase (grout only) and two-phase (grout and water) flow mechanisms (Zou et al., 2018). Zou et al. (2019) incorporated two-phase flow to assess the influence of groundwater on grout propagation, showing that neglecting water flow can overestimate grout penetration length. Zou et al. (2024) numerically simulated grout flow in realistic 3D rough-walled fracture models. Their work displays a peak transmissivity within a specific range of Reynolds number for non-Newtonian fluids, and that surface roughness significantly impacts these flow behaviours. Furthermore, to consider the effect of grout hardening, Yin et al. (2024) used the FDEM-based grouting simulator to explicitly consider the time-dependent rheological characteristics and HM coupling, suggesting a significant impact of decreasing cement-sodium silicate ratio on the penetration range.

Moving to the fracture network scale, DFN models, often coupled with flow simulators, are used to understand how grout propagates through interconnected fractures. Randomised network structures and uncorrelated heterogeneous apertures can delay propagation and increase variability in penetration volume (Zou et al., 2019). The fracture network scale also allows consideration of filtration phenomena at different network constrictions and studying how these lead to grout stoppage (Mohajerani et al., 2017). Most importantly, this scale enables the use of statistical analyses on multiple realisations of fracture networks to quantify uncertainty associated with grout propagation predictions due to the inherent variability of geological formations. At a larger rock mass scale, computational models may employ continuum approaches or upscale properties derived from fracture network models (Ann Emmelin et al., 2007). While these models might not explicitly resolve individual fractures, they provide an overall assessment of the reduced permeability and the improved mechanical properties of rock masses.

4.3. Numerical challenges and improvements

Different computational methodologies possess unique strengths and limitations. The best choice depends on the specific problem, the level of detail desired, and available computational resources. A significant challenge is that most existing computational methods oversimplify grout rheological properties to fit continuum fluid mechanics equations (Lavrov, 2023). Accurately modelling grout's yield stress and time-dependent viscosity remains complex. To address thixotropy without diverse idealizations, Zang et al. (2024) used particulate modelling in a rotational vane system (in Fig. 16a) to capture interparticle bond formation and rupture. Their work revealing local anisotropic flow (Fig. 16b) contrasting with uniform velocity assumptions in continuum models. DEM offers potential for overcoming rheological uncertainties and modelling physical clogging and particle nucleation (time-dependent behaviour) during grout injection. However, DEM's high computational cost remains a bottleneck for upscaling to real-world applications.

Accurately characterising fracture networks in computational models is highly challenging. Rock fractures exhibit irregular and diverse morphologies; indirect methods such as hydraulic measurements can lose crucial roughness/aperture details. Simulating realistic 3D networks with complex grout behaviour and HM coupling is computationally demanding. Consequently, many models still primarily focus on single fractures or 2D networks. The development of more computationally efficient algorithms for large-scale 3D systems remains a focus of ongoing research.

Persistent difficulties exist in model validation and uncertainty quantification. Validating computational models against real-world field data is challenging due to the inherent invisibility of grout flow beneath the surface and the overall complexity of actual field conditions. There is often significant uncertainty associated with the input parameters for computational models, arising from constitutive model choices and the simplification of physical phenomena (e.g., H-M coupling, grout hardening, and filtration). Consequently, deterministic predictions of grout diffusion often have limited reliability, which requires more cautious selection of probability distributions and validation of probabilistic outputs.

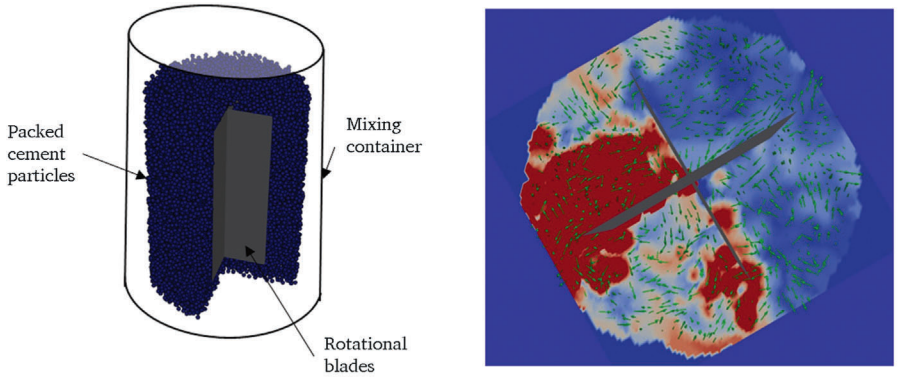

(a) Numerical models of packed cement particles in a rotational vane system

(b) Local anisotropic behaviour represented by complex velocity profiles at the cross-section; green arrows indicate the flow directions of particles, map colour from blue to red indicate the increasing velocity magnitudes

Fig. 16. DEM modelling of grout particles flowing in a rotational vane system, modified after (Zang et al., 2024).

5. Conclusion and future work

This review has critically examined the current state of knowledge and persistent challenges in understanding grout diffusion mechanism within rock fractures. It delves into recent theoretical, experimental, and numerical advancements that address complex grouting diffusion mechanism, ranging from the microscopic interactions of grout particles to continuum descriptions in single fractures and fracture networks. The key conclusions are:

- Grout flow in rock fractures is profoundly influenced by fracture network heterogeneity and the grout's complex non-Newtonian rheology. A comprehensive understanding requires considering both continuum and particulate views.
- Theoretical models provide foundational principles but are often limited to idealized conditions, struggling with complexities like time-dependent rheology, varying apertures, fracture roughness, and hydro-mechanical (HM) coupling.
- Experimental methods have significantly evolved, moving from simplified tests to more realistic simulations with advanced monitoring (e.g., acoustic emission, electrical resistivity, nuclear magnetic resonance) and specialized apparatus. However, fully replicating true in-situ complexities, including HM coupling and diverse fracture network characteristics, remains a substantial limitation.
- Numerical modellings enable dynamic, continuous solutions for complex fracture networks and provide insights into the effects of network characteristics, HM coupling, and non-Newtonian grout properties. Different computational methodologies have unique strengths and limitations regarding detail and computational cost.

Based on current knowledge, recommended future work includes:

- Establish a robust quantitative link between particulate-level grout behaviour (e.g., clogging, filtration, interparticle bonding) and continuum rheological parameters (e.g., yield stress, viscosity). This includes explicitly explaining flow stoppage due to particle blockage in non-Newtonian models.
- Develop improved theoretical models that explicitly incorporate fracture roughness, HM coupling, two-phase flow (grout-water interaction), and time-dependent rheology. Validating existing theoretical assumptions for non-Newtonian flow in rough fractures is also crucial. Furthermore, continuously develop laboratory setups that can better replicate complex in-situ conditions.
- Prioritize computationally modelling complex, realistic grout rheology, including thixotropy and hydration, potentially leveraging DEM to overcome current oversimplifications and high computational costs for upscaling. Improving model validation techniques against real-world field data should be a key focus, especially given the inherent invisibility of grout flow beneath the surface.

CRediT authorship contribution statement

Haizhi Zang: Writing – original draft, Software, Methodology, Formal analysis, Data curation, Conceptualization. **Shanyong Wang:** Writing – review & editing, Supervision, Resources, Investigation, Funding acquisition.

Declaration of competing interest

The authors declare that they have no known competing financial interests or personal relationships that could have appeared to influence the work reported in this paper.

Acknowledgements

The authors are grateful for the financial support provided by the Australian Research Council (ARC) Discovery Project (Grant Nos., DP210100437 and DP230100126) and ARC Linkage Project (Grant No. LP230201048).

References

Al Kuisi, M., Ali, El Naqa, Shaqou, Fathi, 2005. Improvement of dam foundation using grouting intensity number (GIN) technique at tannur dam site, south Jordan. Appl. Sci. 10, 1–16.

Ann Emmelin, M.B., Eriksson, Magnus, Gustafson, Gunnar, Stille, Hakan, 2007. Rock Grouting—Current Competence and Evelopment for the Final Repository. Swedish Nuclear Fuel and Waste Management Co. https://www.osti.gov/etdeweb/biblio/922525.

Azadi, M.R., Taghichian, A., Taheri, A., 2017. Optimization of cement-based grouts using chemical additives. J. Rock Mech. Geotech. Eng. 9 (4), 623–637. https://doi.org/10.1016/j.jrmge.2016.11.013.

Barton, N., Quadros, E., 2019. Understanding the need for pre-injection from permeability measurements: what is the connection? J. Rock Mech. Geotech. Eng. 11 (3), 576–597. https://doi.org/10.1016/j.jrmge.2018.12.008.

Barton, N., Wang, C.S., Yong, R., 2023. Advances in joint roughness coefficient (JRC) and its engineering applications. J. Rock Mech. Geotech. Eng. 15 (12), 3352–3379. https://doi.org/10.1016/j.jrmge.2023.02.002.

Berre, I., Doster, F., Keilegavlen, E., 2019. Flow in fractured porous media: a review of conceptual models and discretization approaches. Transport Porous Media 130 (1), 215–236. https://doi.org/10.1007/s11242-018-1171-6.

Bhasin, R., Johansen, P.M., Barton, N., Makurat, A., 2002. Rock joint sealing experiments using an ultra fine cement grout. In: Ozdemir, L. (Ed.), North American Tunneling 2002. CRC Press, London, pp. 257–262.

Bo, L., Liu, R.R., Zou, L.C., 2024. Theoretical, experimental and numerical analysis of fundamental flow laws of grout in single rock fractures. Rock Soil Mech. 45, 751–760. https://doi.org/10.16285/j.rsm.2023.0700.

Brantberger, M., Stille, H., Eriksson, M., 2000. Controlling grout spreading in tunnel grouting - analyses and developments of the GIN-method. Tunn. Undergr. Space Technol. 15 (4), 343–352. https://doi.org/10.1016/S0886-7798(01)00003-7.

Burgos, G.R., Alexandrou, A.N., Entov, V., 1999. On the determination of yield surfaces in Herschel-Bulkley fluids. J. Rheol. 43 (3), 463–483. https://doi.org/10.1122/1.550992.

Carter, T.G., Dershowitz, W., Shuttle, D., Jefferies, M., 2012. Improved methods of design for grouting fractured rock. In: Johnsen, L.F., Bruce, D.A., Byle, M.J. (Eds.), Grouting and Deep Mixing. American Society of Civil Engineers, Reston, pp. 1472–1483, 2012.

Chen, Z., Zhou, Y.J., Zhang, L.M., Xu, Y.N., 2024. Study on seepage characteristics of grouting slurry for water-absorbing mudstone with rough fissure. Materials 17 (4). https://doi.org/10.3390/ma17040784.

Cui, W., Wang, L., Jiang, Z., Wang, C., Wang, X., Zhang, S., 2021. Numerical Simulation of grouting process in rock mass with rough fracture network based on corrected cubic law. Rock Soil Mech. 42 (8), 8. https://rocksoilmech.researchcommons.org/journal/vol42/iss8/8/.

Dai, G., Bird, R.B., 1981. Radial flow of a Bingham fluid between two fixed circular disks. J. Non-Newton Fluid 8 (3–4), 349–355. https://doi.org/10.1016/0377-0257(81)80031-6.

Deng, S., Wang, X., Yu, J., Zhang, Y., Liu, Z., Zhu, Y., 2018. Simulation of grouting process in rock masses under a dam foundation characterized by a 3D fracture network. Rock Mech. Rock Eng. 51 (6), 1801–1822. https://doi.org/10.1007/s00603-018-1436-y.

Ding, W.Q., Duan, C., Zhang, Q.Z., 2020. Experimental and numerical study on a grouting diffusion model of a single rough fracture in rock mass. Appl. Sci-Basel 10 (20). https://doi.org/10.3390/app10207041.

Dinkgreve, M., Paredes, J., Denn, M.M., Bonn, D., 2016. On different ways of measuring "the" yield stress. J. Non-Newton Fluid 238, 233–241. https://doi.org/10.1016/j.jnnfm.2016.11.001.

Draganovic, A., Stille, H., 2014. Filtration of cement-based grouts measured using a long slot. Tunn. Undergr. Space Technol. 43, 101–112. https://doi.org/10.1016/j.tust.2014.04.010.

Du, X.M., Fang, H.Y., Wang, S.Y., Xue, B.H., Wang, F.M., 2021. Experimental and practical investigation of the sealing efficiency of cement grouting in tortuous fractures with flowing water. Tunn. Undergr. Space Technol. 108, 103693. https://doi.org/10.1016/j.tust.2020.103693.

Duan, H.Y., Ma, D., Zou, L.C., Xie, S.J., Liu, Y., 2024. Co-exploitation of coal and geothermal energy through water-conducting structures: improving extraction efficiency of geothermal well. Renew. Energy 228. https://doi.org/10.1016/j.renene.2024.120666.

Duan, H.Y., Xie, Y.S., Zou, L.C., Li, B., Håkansson, U., Cvetkovic, V., 2025. Analysis of grout radial propagation in water-saturated rough-walled rock fractures. Int. J. Rock Mech. Min. Sci. 190. https://doi.org/10.1016/j.ijrmms.2025.106101.

Dzuy, N.Q., Boger, D.V., 1983. Yield stress measurement for concentrated suspensions. J. Rheol. 27 (4), 321–349. https://doi.org/10.1122/1.549709.

Eklund, D., Stille, H., 2008. Penetrability due to filtration tendency of cement-based grouts. Tunn. Undergr. Space Technol. 23 (4), 389–398. https://doi.org/10.1016/j.tust.2007.06.011.

El Mohtar, C., Jaffal, H., Miller, A.K., Ward, K., 2022. Implementing digital imaging for improved understanding of microfine cement grout permeation and filtration. Geotech. Geol. Eng. 40 (9), 4473–4485. https://doi.org/10.1007/s10706-022-02164-z.

El Tani, M., 2012. Grouting rock fractures with cement grout. Rock Mech. Rock Eng. 45 (4), 547–561. https://doi.org/10.1007/s00603-012-0235-0.

El Tani, M., Lopez-Molina, J., 2020. Running limit and refusal in rock fractures grouting. Rock Mech. Rock Eng. 53 (5), 2201–2214. https://doi.org/10.1007/s00603-019-02024-y.

Eriksson, M., 2002. Prediction of Grout Spread and Sealing Effect. KTH Royal Institute of Technology. Doctoral thesis.

Eriksson, M., Friedrich, M., Vorschulze, C., 2004. Variations in the rheology and penetrability of cement-based grouts—an experimental study. Cement Concr. Res. 34 (7), 1111–1119. https://doi.org/10.1016/j.cemconres.2003.11.023.

Fan, Q., Jiang, X., Wang, K., Huang, C., Li, G., Wei, P., 2023. Cement grouting online monitoring and intelligent control for dam foundations. J. Intell. Constr. 1 (1), 1–15. https://doi.org/10.26599/JIC.2023.9180005.

Fransson, A., Tsang, C.F., Rutqvist, J., Gustafson, G., 2007. A new parameter to assess hydromechanical effects in single-hole hydraulic testing and grouting. Int. J. Rock Mech. Min. Sci. 44 (7), 1011–1021. https://doi.org/10.1016/j.ijrmms.2007.02.007.

Funehag, J., Thörn, J., 2018. Radial penetration of cementitious grout–Laboratory verification of grout spread in a fracture model. Tunn. Undergr. Space Technol. 72, 228–232. https://doi.org/10.1016/j.tust.2017.11.020.

Gao, H., Qing, L.B., Ma, G.W., Zhang, D.C., Wei, C.L., 2024. Numerical investigation into effects of rheological properties on grout flow in rock fracture using Herschel-Bulkley model. Eng. Geol. 329, 107402. https://doi.org/10.1016/j.enggeo.2023.107402.

Ghafar, A.N., Mentesidis, A., Draganovic, A., Larsson, S., 2016. An experimental approach to the development of dynamic pressure to improve grout spread. Rock Mech. Rock Eng. 49 (9), 3709–3721. https://doi.org/10.1007/s00603-016-1020-2.

Ghafar, A.N., Sadrizadeh, S., Draganovic, A., Johansson, F., Håkansson, U., Larsson, S., 2017a. Application of low-frequency rectangular pressure impulse in rock grouting. In: Gazzarrini, P., R, T.D., Bruce, D.A., Byle, M.J., Mohtar, C.S.E., Johnsen, L.F. (Eds.), Grouting 2017. American Society of Civil Engineers, Reston, pp. 104–113.

Ghafar, A.N., Sadrizadeh, S., Magakis, K., Draganovic, A., Larsson, S., 2017b. Varying aperture long slot (VALS), a method for studying grout penetrability into fractured hard rock. Geotech. Test. J. 40 (5), 871–882. https://doi.org/10.1520/Gtj20160179.

Gothäll, R., Stille, H., 2010. Fracture–fracture interaction during grouting. Tunn. Undergr. Space Technol. 25 (3), 199–204. https://doi.org/10.1016/j.tust.2009.11.003.

Gustafson, G., Claesson, J., Fransson, A., 2013. Steering parameters for rock grouting. J. Appl. Math. https://doi.org/10.1155/2013/269594.

Han, C.H., Zhang, W.J., Zhou, W.W., Guo, J.B., Yang, F., Man, X.Q., Jiang, J.G., Zhang, C. R., Li, Y.J., Wang, Z., Wang, H., 2020. Experimental investigation of the fracture grouting efficiency with consideration of the viscosity variation under dynamic pressure conditions. Carbonates Evaporites 35 (2). https://doi.org/10.1007/s13146-020-00568-7.

Han, C.H., Wei, J.C., Zhang, W.J., Zhou, W.W., Yin, H.Y., Xie, D.L., Yang, F., Li, X., Man, X.Q., 2021. Numerical investigation of grout diffusion accounting for the dynamic pressure boundary condition and spatiotemporal variation in slurry viscosity. Int. J. GeoMech. 21 (4). https://doi.org/10.1061/(Asce)Gm.1943-5622.0001945.

Hao, M., El Tani, M., Li, X., 2023. Analytical solution for expandable polyurethane grouting in a rock fracture. Rev. Fr. Geotech. 174, 4. https://doi.org/10.1051/geotech/2023018.

Hassler, L., Hakansson, U., Stille, H., 1992. Computer-simulated flow of grouts in jointed rock. Tunn. Undergr. Space Technol. 7 (4), 441–446. https://doi.org/10.1016/0886-7798(92)90074-R.

Henderson, A.E., Robertson, I.A., Whitfield, J.M., Garrard, G.F.G., Swannell, N.G., Fisch, H., 2008. A new method for real-time monitoring of grout spread through fractured rocks. Materials Research Society Symposium Proceedings. https://doi.org/10.1557/Proc-1107-577.

Hu, C., Guo, J., Wang, Z., 2022. Lattice Boltzmann simulation for grout filling process during simultaneous backfill grouting of shield in tunnel construction. Eur. J. Environ. Civ. Eng. 26 (9), 4039–4054. https://doi.org/10.1080/19648189.2020.1837251.

Jiang, D.H., Cheng, X.Z., Luan, H.J., Wang, T.X., Zhang, M.G., Hao, R.Y., 2018. Experimental investigation on the law of grout diffusion in fractured porous rock mass and its application. Processes 6 (10). https://doi.org/10.3390/pr6100191.

Jin, L., Sui, W., 2021. Experimental investigation on chemical grouting in rough 2D fracture network with flowing water. Bull. Eng. Geol. Environ. 80 (11), 8519–8533. https://doi.org/10.1007/s10064-021-02448-3.

Kang, H., Li, W., Gao, F., Yang, J., 2023. Grouting theories and technologies for the reinforcement of fractured rocks surrounding deep roadways. Deep Undergr. Sci. Eng. 2 (1), 2–19. https://doi.org/10.1002/dug2.12026.

Kobayashi, S., Stille, H., 2007. Design for Rock Grouting Based on Analysis of Grout Penetration. Verification Using Äspö HRL Data and Parameter Analysis. Swedish Nuclear Fuel and Waste Management Co.

Kvartsberg, S., 2013. On the use of engineering geological information in rock grouting design. Befo Report 125, 1–88.

Larson, R.G., Wei, Y.F., 2019. A review of thixotropy and its rheological modeling. J Rheol 63 (3), 477–501. https://doi.org/10.1122/1.5055031.

Latham, J.-P., Xiang, J., Belayneh, M., Nick, H.M., Tsang, C.-F., Blunt, M.J., 2013. Modelling stress-dependent permeability in fractured rock including effects of propagating and bending fractures. Int. J. Rock Mech. Min. Sci. 57, 100–112. https://doi.org/10.1016/j.ijrmms.2012.08.002.

Lavrov, A., 2023. Flow of non-Newtonian fluids in single fractures and fracture networks: current status, challenges, and knowledge gaps. Eng. Geol. 321. https://doi.org/10.1016/j.enggeo.2023.107166.

Lee, H., Oh, T.M., Lee, J.W., 2021. Evaluation of grout penetration in single rock fracture using electrical resistivity. Geomech. Eng. 24 (1), 1–14. https://doi.org/10.12989/gae.2021.24.1.001.

Lee, J.W., Kim, H.M., Yazdani, M., Lee, H., Oh, T.M., Park, E.S., 2019. Experimental observation and numerical simulation of cement grout penetration in discrete joints. Geomech. Eng. 18 (3), 259–266. https://doi.org/10.12989/gae.2019.18.3.259.

Lei, Q., Latham, J.-P., Tsang, C.-F., 2017. The use of discrete fracture networks for modelling coupled geomechanical and hydrological behaviour of fractured rocks. Comput. Geotech. 85, 151–176. https://doi.org/10.1016/j.compgeo.2016.12.024.

Lei, Q., Gholizadeh Doonechaly, N., Tsang, C.-F., 2021. Modelling fluid injection-induced fracture activation, damage growth, seismicity occurrence and connectivity change in naturally fractured rocks. Int. J. Rock Mech. Min. Sci. 138. https://doi.org/10.1016/j.ijrmms.2020.104598.

Li, G.S., Li, Z.H., Du, F., Cao, Z.Z., Wang, W.Q., 2024. Development of grouting test system for rough fissure rock body and research on slurry diffusion law. Appl. Sci-Basel 14 (1). https://doi.org/10.3390/app14010047.

Liang, J.S., Du, X.M., Fang, H.Y., Li, B., Zhao, X.H., Xue, B.H., Zhai, K.J., Wang, S.Y., 2024. Numerical manifold simulation and medium-parameter analysis of the polymer grouting process in three-dimensional rock fractures. Comput. Geotech. 173. https://doi.org/10.1016/j.compgeo.2024.106586.

Liang, Y.K., Sui, W.H., Qi, J.F., 2019. Experimental investigation on chemical grouting of inclined fracture to control sand and water flow. Tunn. Undergr. Space Technol. 83, 82–90. https://doi.org/10.1016/j.tust.2018.09.038.

Liu, B., Sang, H.M., Liu, Q.S., Kang, Y.S., Pan, Y.C., Lu, C.B., Zhang, C.Q., 2020a. New algorithm for simulating grout diffusion and migration in fractured rock masses. Int. J. GeoMech. 20 (3). https://doi.org/10.1061/(Asce)Gm.1943-5622.0001537.

Liu, B., Sang, H.M., Liu, Q.S., Liu, H., Pan, Y.C., Kang, Y.S., 2021. Laboratory study on diffusion and migration of grout in rock mass fracture network. Int. J. GeoMech. 21 (1). https://doi.org/10.1061/(Asce)Gm.1943-5622.0001901.

Liu, C., Huang, X., Yue, W., Zhang, C., 2020b. Extension of grouting-induced splitting fractures in materials similar to coal rocks containing prefabricated fractures. J. Geophys. Eng. 17 (4), 670–685. https://doi.org/10.1093/jge/gxaa021.

Liu, Q., Sun, L., 2019. Simulation of coupled hydro-mechanical interactions during grouting process in fractured media based on the combined finite-discrete element method. Tunn. Undergr. Space Technol. 84, 472–486. https://doi.org/10.1016/j.tust.2018.11.018.

Liu, W., Park, J.M., 2020. Discussion on "Analysis of Bingham fluid radial flow in smooth fractures". J. Rock Mech. Geotech. Eng. 12, 1112–1118. https://doi.org/10.1016/j.jrmge.2021.03.001. J. Rock Mech. Geotech. Eng. 2021;13(4): 937-944.

Lu, Y., He, M., Wang, L., Ren, B., Sun, X., Zhang, K., 2020. In-situ visualization experiments on the microscopic process of particle filtration of cement grouts within a rock fracture. Tunn. Undergr. Space Technol. 95, 103157. https://doi.org/10.1016/j.tust.2019.103157.

Ma, G.W., Wang, Z.H., Wang, H.D., 2025. Grouting geological model (GGM): definition, characterization, modeling, and application in determining grouting material and pressure. Rock Mech. Rock Eng. https://doi.org/10.1007/s00603-024-04369-5.

Meng, B., 2021. State of the Art Report on Cement Based Grout Properties and Dynamic Grouting. KTH Royal Institute of Technology. Master thesis.

Mohajerani, S., Baghbanan, A., Wang, G., Forouhandeh, S.F., 2017. An efficient algorithm for simulating grout propagation in 2D discrete fracture networks. Int. J. Rock Mech. Min. Sci. 98, 67–77. https://doi.org/10.1016/j.ijrmms.2017.07.015.

Mohammed, M.H., Pusch, R., Knutsson, S., 2015. Study of cement-grout penetration into fractures under static and oscillatory conditions. Tunn. Undergr. Space Technol. 45, 10–19. https://doi.org/10.1016/j.tust.2014.08.003.

Nazempour, M.M., Majdi, A., 2021. An analytical method of predicting length of grout penetration in jointed rocks. J Min Environ 12 (4), 1153–1173. https://doi.org/10.22044/jme.2022.11435.2127.

Nejad Ghafar, A., Draganovic, A., Larsson, S., 2015. An experimental study of the influence of dynamic pressure on improving grout penetrability. Befo Report 149, 1–96.

Nejad Ghafar, A., Ali Akbar, S., Al-Naddaf, M., Draganovic, A., Larsson, S., 2017. Uncertainties in grout penetrability measurements; evaluation and comparison of filter pump, penetrability meter and short slot. Geotech. Geol. Eng. https://doi.org/10.1007/s10706-017-0351-4.

Ortega, J.L.V., Vergara, A.I.G., 2024. Simulation of expansion and contraction for sudden plastic flow of Bingham cement grout and Newtonian fluids in a rectangular duct, using the lattice Boltzmann method. Heliyon 10 (6), e28151. https://doi.org/10.1016/j.heliyon.2024.e28151.

Papanastasiou, T.C., Boudouvis, A.G., 1997. Flows of viscoplastic materials: models and computations. Comput. Struct. 64 (1–4), 677–694. https://doi.org/10.1016/S0045-7949(96)00167-8.

Park, J.M., 2020. Flow classification of radial and squeeze flows between parallel disks. J. Non-Newton Fluid 286. https://doi.org/10.1016/j.jnnfm.2020.104416.

Park, J.M., Lim, K., 2023. Diverging radial flow of a viscoplastic fluid in narrow gaps of varying thickness. J. Non-Newton Fluid 316. https://doi.org/10.1016/j.jnnfm.2023.105031.

Rafi, J., Stille, H., 2021. A method for determining grouting pressure and stop criteria to control grout spread distance and fracture dilation. Tunn. Undergr. Space Technol. 112. https://doi.org/10.1016/j.tust.2021.103885.

Rafi, J.Y., Stille, H., 2014. Control of rock jacking considering spread of grout and grouting pressure. Tunn. Undergr. Space Technol. 40, 1–15. https://doi.org/10.1016/j.tust.2013.09.005.

Rafi, J.Y., Stille, H., 2015. Basic mechanism of elastic jacking and impact of fracture aperture change on grout spread, transmissivity and penetrability. Tunn. Undergr. Space Technol. 49, 174–187. https://doi.org/10.1016/j.tust.2015.04.002.

Rahman, M., Håkansson, U., Wiklund, J., 2015. In-line rheological measurements of cement grouts: effects of water/cement ratio and hydration. Tunn. Undergr. Space Technol. 45, 34–42. https://doi.org/10.1016/j.tust.2014.09.003.

Rahman, M., Wiklund, J., Kotze, R., Hakansson, U., 2017. Yield stress of cement grouts. Tunn. Undergr. Space Technol. 61, 50–60. https://doi.org/10.1016/j.tust.2016.09.009.

Ramskill, N.P., Sederman, A.J., Mantle, M.D., Appel, M., de Jong, H., Gladden, L.F., 2018. In situ chemically-selective monitoring of multiphase displacement processes in a carbonate rock using 3D. Magnetic Reson. Imaging. Transp. Porous Media 121 (1), 15–35. https://doi.org/10.1007/s11242-017-0945-6.

Ren, Y., Du, F., Chen, H., Hong, Z., Ren, Z., 2022. Migration characteristics and restoration mechanism of grout containing aggregate in overburden fractures based on CFD-DEM coupling model. Geofluids 2022, 1–11. https://doi.org/10.1155/2022/3254660.

Roussel, N., Ovarlez, G., Garrault, S., Brumaud, C., 2012. The origins of thixotropy of fresh cement pastes. Cement Concr. Res. 42 (1), 148–157. https://doi.org/10.1016/j.cemconres.2011.09.004.

Roussel, N., Bessaies-Bey, H., Kawashima, S., Marchon, D., Vasilic, K., Wolfs, R., 2019. Recent advances on yield stress and elasticity of fresh cement-based materials. Cement Concr. Res. 124, 105798. https://doi.org/10.1016/j.cemconres.2019.105798.

Rutqvist, J., Stephansson, O., 2003. The role of hydromechanical coupling in fractured rock engineering. Hydrogeol. J. 11 (1), 7–40. https://doi.org/10.1007/s10040-002-0241-5.

Saeidi, O., Stille, H., Torabi, S.R., 2013. Numerical and analytical analyses of the effects of different joint and grout properties on the rock mass groutability. Tunn. Undergr. Space Technol. 38, 11–25. https://doi.org/10.1016/j.tust.2013.05.005.

Shamu, T.J., Zou, L.C., Kotze, R., Wiklund, J., Hakansson, U., 2020. Radial flow velocity profiles of a yield stress fluid between smooth parallel disks. Rheol. Acta 59 (4), 239–254. https://doi.org/10.1007/s00397-020-01203-x.

Shamu, T.J., Zou, L.C., Hakansson, U., 2021. A nomogram for cement-based rock grouting. Tunn. Undergr. Space Technol. 116. https://doi.org/10.1016/j.tust.2021.104110.

Si, X.F., Zhang, Z.L., Li, X.B., Yi, G.S., Luo, Y., Tan, L.H., Han, K.F., 2025. Influences of maximum principal stress direction and cross-section shape on tunnel stability. J. Rock Mech. Geotech. Eng. 17 (4), 2159–2180. https://doi.org/10.1016/j.jrmge.2024.10.003.

Singh, K.K., Singh, D.N., Ranjith, P.G., 2015. Laboratory simulation of flow through single fractured granite. Rock Mech. Rock Eng. 48 (3), 987–1000. https://doi.org/10.1007/s00603-014-0630-9.

Sun, L., Grasselli, G., Liu, Q., Tang, X., 2019. Coupled hydro-mechanical analysis for grout penetration in fractured rocks using the finite-discrete element method. Int. J. Rock Mech. Min. Sci. 124. https://doi.org/10.1016/j.ijrmms.2019.104138.

Sun, L., Li, M., Abdelaziz, A., Tang, X., Liu, Q., Grasselli, G., 2023. An efficient 3D cell-based discrete fracture-matrix flow model for digitally captured fracture networks. Int. J. Coal Sci. Technol. 10 (1), 70. https://doi.org/10.1007/s40789-023-00625-1.

Tong, F., Yang, J., Duan, M.Q., Ma, X.F., Li, G.C., 2022. The numerical simulation of rock mass grouting: a literature review. Eng Computation 39 (5), 1902–1921. https://doi.org/10.1108/Ec-05-2021-0282.

Trinchero, P., Zou, L.C., de la Iglesia, M., Iraola, A., Bruines, P., Deissmann, G., 2024. Experimental and numerical analysis of flow through a natural rough fracture subject to normal loading. Sci. Rep. 14 (1). https://doi.org/10.1038/s41598-024-55751-w.

Viswanathan, H.S., Ajo-Franklin, J., Birkholzer, J.T., Carey, J.W., Guglielmi, Y., Hyman, J.D., Karra, S., Pyrak-Nolte, L.J., Rajaram, H., Srinivasan, G., Tartakovsky, D.M., 2022. From fluid flow to coupled processes in fractured rock: recent advances and new frontiers. Rev. Geophys. 60 (1). https://doi.org/10.1029/2021rg000744.

Wang, X.C., Xiao, F., Zhang, Q.S., Zhou, A.N., Liu, R.T., 2021. Grouting characteristics in rock fractures with rough surfaces: apparatus design and experimental study. Measurement 184. https://doi.org/10.1016/j.measurement.2021.109870.

Wang, Y.H., Yang, P., Li, Z.T., Wu, S.J., Zhao, Z.X., 2020. Experimental-numerical investigation on grout diffusion and washout in rough rock fractures under flowing water. Comput. Geotech. 126. https://doi.org/10.1016/j.compgeo.2020.103717.

Weng, L., Wu, Z.J., Zhang, S.L., Liu, Q.S., Chu, Z.F., 2022. Real-time characterization of the grouting diffusion process in fractured sandstone based on the low-field nuclear magnetic resonance technique. Int. J. Rock Mech. Min. Sci. 152. https://doi.org/10.1016/j.ijrmms.2022.105060.

Widmann, R., 1996. International society for rock mechanics commission on rock grouting. Int. J. Rock Mech. Min. Sci. Geomech. Abstr. 33 (8), 803–847. https://doi.org/10.1016/S0148-9062(96)00015-0.

Xiang, Z., Zhang, N., Xie, Z., Tang, H., Song, Z., 2025. Experimental study on permeation of composite grout with multi-particle-size distribution: comparative analysis with nano-silica sol and cement grout. Processes 13 (1). https://doi.org/10.3390/pr13010172.

Xiao, F., Shang, J.L., Zhao, Z.Y., 2019. DDA based grouting prediction and linkage between fracture aperture distribution and grouting characteristics. Comput. Geotech. 112, 350–369. https://doi.org/10.1016/j.compgeo.2019.04.028.

Yaghoobi Rafi, J., 2014. Study of Pumping Pressure and Stop Criteria in Grouting of Rock Fractures. KTH Royal Institute of Technology. Doctorate thesis.

Yang, P., Liu, Y.H., Gao, S.W., Xue, S.B., 2020. Experimental investigation on the diffusion of carbon fibre composite grouts in rough fractures with flowing water. Tunn. Undergr. Space Technol. 95. https://doi.org/10.1016/j.tust.2019.103146.

Yin, X., Wu, Z., Xu, X., Weng, L., Liu, Q., 2024. Numerical investigation on the grouting penetration process of quick-setting grout in discrete fractured rock mass based on the combined finite–discrete-element method. Int. J. GeoMech. 24 (3), 04023298. https://doi.org/10.1061/IJGNAI.GMENG-9247.

Zang, H.Z., Wang, S.Y., Carter, J.P., 2024. Analysis of thixotropy of cement grout based on a virtual bond model. Acta Geotech 19 (11), 7427–7450. https://doi.org/10.1007/s11440-024-02417-6.

Zang, H.Z., Wang, S.Y., Carter, J.P., 2025. Forward and inverse models of magnetically-susceptible grout in rock fracture grouting. Acta Geotech. https://doi.org/10.1007/s11440-024-02491-w.

Zhang, Q.S., Zhang, L.Z., Liu, R.T., Li, S.C., Zhang, Q.Q., 2017. Grouting mechanism of quick setting slurry in rock fissure with consideration of viscosity variation with space. Tunn. Undergr. Space Technol. 70, 262–273. https://doi.org/10.1016/j.tust.2017.08.016.

Zhang, S.H., Aberg, W., Johansson, F., Funehag, J., Zou, L.C., 2025. Experimental study on erosion and viscous fingering of fresh cement-based grout after injection stops. Rock Mech. Rock Eng. https://doi.org/10.1007/s00603-025-04486-9.

Zhou, L., Su, K., Wu, H.G., Shi, C.Z., 2018. Numerical investigation of grouting of rock mass with fracture propagation using cohesive finite elements. Int. J. GeoMech. 18 (7). https://doi.org/10.1061/(Asce)Gm.1943-5622.0001184.

Zhu, G.X., Zhang, Q.S., Lin, X., Liu, R.T., Zhang, L.Z., Zhang, J.W., 2020. Analysis of the sealing mechanism of cement-sodium silicate grout in rock fractures with flowing water. Water 12 (7). https://doi.org/10.3390/w12071935.

Zhu, Y.S., Wang, X.L., Deng, S.H., Chen, W.L., Shi, Z.Z., Xue, L.L., Lv, M.M., 2019. Grouting process simulation based on 3D fracture network considering fluid-structure interaction. Appl. Sci.-Basel. 9 (4). https://doi.org/10.3390/app9040667.

Zimmerman, R.W., Bodvarsson, G.S., 1996. Hydraulic conductivity of rock fractures. Transport Porous Media 23, 1–30. https://doi.org/10.1007/BF00145263.

Zou, L., Håkansson, U., Cvetkovic, V., 2020a. Analysis of Bingham fluid radial flow in smooth fractures. J. Rock Mech. Geotech. Eng. 12 (5), 1112–1118. https://doi.org/10.1016/j.jrmge.2019.12.021.
Zou, L., Håkansson, U., Cvetkovic, V., 2021. Analysis of cement grout propagation in fractured rocks. Befo Report 200, 1–62.
Zou, L.C., Hakansson, U., Cvetkovic, V., 2018. Two-phase cement grout propagation in homogeneous water-saturated rock fractures. Int. J. Rock Mech. Min. Sci. 106, 243–249. https://doi.org/10.1016/j.ijrmms.2018.04.017.
Zou, L.C., Hakansson, U., Cvetkovic, V., 2019. Cement grout propagation in two-dimensional fracture networks: impact of structure and hydraulic variability. Int. J. Rock Mech. Min. Sci. 115, 1–10. https://doi.org/10.1016/j.ijrmms.2019.01.004.
Zou, L.C., Hakansson, U., Cvetkovic, V., 2020b. Yield-power-law fluid propagation in water-saturated fracture networks with application to rock grouting. Tunn. Undergr. Space Technol. 95. https://doi.org/10.1016/j.tust.2019.103170.
Zou, L.C., Tang, M., Li, B., 2024. Bingham and herschel-bulkley fluids flow regimes in rough-walled rock fractures. Int. J. Rock Mech. Min. Sci. 180. https://doi.org/10.1016/j.ijrmms.2024.105832.